RESEARCH ARTICLE

AMERICAN JOURNAL OF BOTANY

Seed morphology and anatomy and its utility in recognizing subfamilies and tribes of Zingiberaceae[1]

John C. Benedict[2,10], Selena Y. Smith[2,3], Margaret E. Collinson[4], Jana Leong-Škorničková[5], Chelsea D. Specht[6], Federica Marone[7], Xianghui Xiao[8], and Dilworth Y. Parkinson[9]

PREMISE OF THE STUDY: Recent phylogenetic analyses based on molecular data suggested that the monocot family Zingiberaceae be separated into four subfamilies and four tribes. Robust morphological characters to support these clades are lacking. Seeds were analyzed in a phylogenetic context to test independently the circumscription of clades and to better understand evolution of seed characters within Zingiberaceae.

METHODS: Seventy-five species from three of the four subfamilies were analyzed using synchrotron based x-ray tomographic microscopy (SRXTM) and scored for 39 morphoanatomical characters.

KEY RESULTS: Zingiberaceae seeds are some of the most structurally complex seeds in angiosperms. No single seed character was found to distinguish each subfamily, but combinations of characters were found to differentiate between the subfamilies. Recognition of the tribes based on seeds was possible for Globbeae, but not for Alpinieae, Riedelieae, or Zingibereae, due to considerable variation.

CONCLUSIONS: SRXTM is an excellent, nondestructive tool to capture morphoanatomical variation of seeds and allows for the study of taxa with limited material available. Alpinioideae, Siphonochiloideae, Tamijioideae, and Zingiberoideae are well supported based on both molecular and morphological data, including multiple seed characters. Globbeae are well supported as a distinctive tribe within the Zingiberoideae, but no other tribe could be differentiated using seeds due to considerable homoplasy when compared with currently accepted relationships based on molecular data. Novel seed characters suggest tribal affinities for two currently unplaced Zingiberaceae taxa: *Siliquamomum* may be related to Riedelieae and *Monolophus* to Zingibereae, but further work is needed before formal revision of the family.

KEY WORDS aril; chalaza; embryo; ginger; micropyle; monocotyledon; operculum; seed coat; synchrotron-based x-ray tomographic microscopy (SRXTM); testa

Seeds are an integral part of a plant, but detailed information about them and their utility in phylogenetic studies is limited. In a seminal work on dicotyledonous seed anatomy, Corner (1976: p. vii) stated, "…classification without seed-structure is unsound and, consequently, our knowledge of the evolution of flowering plants." Along with potentially clarifying systematic relationships between taxa, data on seed morphoanatomy are also fundamental to addressing the carpological fossil record, which in turn enlightens our understanding of evolution, paleoecology, paleobiogeography, and past climate change (e.g., Manchester and Kress, 1993; Collinson and van Bergen, 2004; Chen and Manchester, 2007; Collinson et al., 2012; Herrera et al., 2014). Understanding seed structure also enhances our understanding of biological features that may facilitate dispersal, inhibit or facilitate dormancy, and survivability—information particularly relevant to germplasm banks, which strive to preserve biodiversity (e.g., Boesewinkel and Bouman, 1995; Baskin and Baskin, 2001; Wada et al., 2011) and contribute considerably to the proper identification of commercially important or potentially important plants (e.g., Vaughan, 1970; Wu et al., 2014) and food security. Thus, seed anatomical studies are important in a variety of ways.

[1] Manuscript received 23 June 2015; revision accepted 18 September 2015.

[2] Department of Earth and Environmental Sciences, University of Michigan, Ann Arbor, Michigan 48109-1005 USA;
[3] Museum of Paleontology, University of Michigan, Ann Arbor, Michigan 48109-1079 USA;
[4] Department of Earth Sciences, Royal Holloway University of London, London, UK, TW20 0EX;
[5] Herbarium, Singapore Botanic Gardens, National Parks Board, Singapore 259569;
[6] Department of Plant and Microbial Biology, Integrative Biology and the University and Jepson Herbaria, University of California, Berkeley, California 94750-2465 USA;
[7] Swiss Light Source, Paul Scherrer Institut, 5232 Villigen PSI, Switzerland;
[8] Advanced Photon Source, Argonne National Laboratories, Argonne, Illinois 60439 USA; and
[9] Advanced Light Source, Lawrence Berkeley National Laboratories, Berkeley, California 94720 USA
[10] Author for correspondence (e-mail: jcbenedi@umich.edu)
doi:10.3732/ajb.1500300

Zingiberaceae are an economically and ecologically important family of commelinid monocots with a center of diversity in Southeast Asia (Kress et al., 2002; Larsen, 2005). It is the largest and most species-rich family within Zingiberales and currently contains 52 genera and approximately 1600 species, with an average of 13 new taxa being described a year for the past two decades (The Plant List, 2013). Seeds of Zingiberales have been studied for more than a century (Tschirch, 1891; Humphrey, 1896; Netolitzky, 1926; Mauritzon, 1936; Takhtajan, 1985). More recently they have been studied in search of potential pharmacognostical characteristics (see Liao and Wu, 1996 for a review), but little information is available on utilizing seeds as a source of data for systematics and often these studies are limited in scope to a few species or genera (Kimura and Yoshimura, 1968; Liao and Wu, 1996; Wu et al., 2014). Furthermore, many early studies were the subject of interfamilial comparisons based often on immature seeds, which do not demonstrate anatomical differences seen in later stages of development (e.g., Humphrey, 1896; see Takhtajan, 1985 for comparisons). One potential reason for the paucity of studies on zingiberalean seeds is the presence of a hard, brittle seed coat with phytoliths, making traditional paraffin embedding and microtomy difficult (Benedict, 2012; Benedict et al., 2015). The use of synchrotron-based x-ray tomographic microscopy (SRXTM) to analyze the seeds provides high-resolution detail of seed coats and seed and embryo internal morphoanatomy. In addition, SRXTM is nondestructive and requires no specimen-altering preparations (e.g., critical point drying, rehydration, coating), which provides the opportunity to analyze rare material from herbarium specimens and to standardize anatomical observations across a wide range of taxa (Smith et al., 2009; Benedict et al., 2015).

Traditional circumscription of the Zingiberaceae by Schumann (1904), Holttum (1950), Burtt and Smith (1972), and Larsen et al. (1998) included four tribes (Alpinieae, Hedychieae, Globbeae, and Zingibereae). Recent work, based on molecular data, recognizes four subfamilies (Alpinioideae, Siphonochiloideae, Tamijioideae, Zingiberoideae) with tribe Zingibereae, tribe Globbeae, and *Monolophus* (formerly *Caulokaempferia*; Mood et al., 2014) nested within Zingiberoideae, and tribe Alpinieae, tribe Riedelieae, and *Siliquamomum* nested within Alpinioideae (Table 1). Tamijioideae are monospecific and Siphonochiloideae contain two genera (Kress et al., 2002; Table 1). All subfamilies are well supported based on molecular and morphological data, but many speciose genera (e.g., *Alpinia*, *Amomum*, and *Curcuma*) have been shown to be paraphyletic and/or polyphyletic (*Amomum*: Harris et al., 2000; Xia et al., 2004; *Alpinia*: Rangsiruji et al., 2000; Zingibereae: Ngamriabsakul et al., 2004; *Etlingera*: Pedersen, 2004; *Globba*: Williams et al., 2004; Alpinioideae: Kress et al., 2005, 2007; *Curcuma*: Záveská et al., 2012; Leong-Škorničková et al., 2015).

The family as a whole is easily separated from other Zingiberales families by possessing ligulate distichous leaves, flowers with a single dithecal stamen, and an often showy petaloid labellum formed from two or four staminodes (Simpson, 2010). Within Zingiberaceae, the plane of distichy along a leafy shoot separates Alpinioideae (perpendicular to the rhizome) from the other tribes (parallel to rhizome), but many other floral and vegetative characters previously used to distinguish tribes (e.g., locule number, presence/absence of lateral staminodes) are not unique to any particular subfamily or tribe (Kress et al., 2002). A single synapomorphic character was suggested to distinguish Riedelieae from Alpinieae: the presence of extrafloral nectaries approximately 2.5 cm above the petiole on the midrib or costa of the adaxial surface of the leaf (Kress et al., 2002). This character has indeed been documented for all members of Riedelieae (Mood, 1996; Larsen and Mood, 1998; Kress et al., 2002), but it has also been observed in various species of Alpinioideae, e.g., *Amomum citrinum* (Ridl.) Holttum, *Amomum xanthophlebium* Baker, *Hornstedtia sanhan* M.F.Newman, as well in Zingiberoideae, e.g., *Zingiber singapurense* Škorničk. (J. Leong-Škorničková, personal observations) and therefore cannot be used to define Riedelieae. Unfortunately morphological characters useful for distinguishing various clades in Zingiberaceae are exceedingly rare, but are crucial for independently testing phylogenetic hypotheses based on molecular data.

To date, a single preliminary systematic treatment of Zingiberaceae seeds by Liao and Wu (2000) showed that the two main subfamilies can be distinguished based on anatomical details of the endotesta, which is sclerenchymatous in Alpinioideae and parenchymatous with often rectangular cells in Zingiberoideae. While this preliminary study was useful in documenting this distinguishing character between the two subfamilies, it only documented four characters for the 60 taxa analyzed. This is true for many previous studies on Zingiberales seeds where very few seed characters are incorporated into analyses, which limits their application in plant

TABLE 1. Currently recognized subfamilies, tribes, and genera within Zingiberaceae (after Kress et al., 2002; Takano and Nagamasu, 2007; Leong-Škorničková et al., 2011; Mood et al., 2014). Numbers in parentheses indicate currently accepted number of species reported on The Plant List (2013), IPNI (2015), in Mood et al. (2014), or Leong-Škorničková et al. (2015). An asterisk (*) denotes genera described since Kress et al. (2002).

Subfamily Siphonochiloideae	**Subfamily Tamijioideae**	**Subfamily Alpinioideae**	**Subfamily Zingiberoideae**
Tribe	Tribe	Tribe	Tribe
Siphonochileae	**Tamijieae**	**Alpinieae**	**Zingibereae**
Aulotandra (6)	*Tamijia* (1)	*Aframomum* (56)	*Boesenbergia* (69)
Siphonochilus (11)		*Alpinia* (247)	*Camptandra* (4)
		Amomum (180)	*Cautleya* (2)
		Cyphostigma (1)	*Cornukaempferia* (3)
		Elettaria (11)	*Curcuma* (105)
		Elettariopsis (20)	*Distichochlamys* (3)
		Etlingera (100)	*Haniffia* (4)
		Geocharis (6)	*Haplochorema* (6)
		Geostachys (25)	*Hedychium* (95)
		Hornstedtia (34)	*Kaempferia* (36)
		Leptosolena (1)	*Larsenianthus** (4)
		Plagiostachys (27)	*Nanochilus* (1)
		Renealmia (87)	*Newmania** (2)
		Vanoverberghia (2)	*Myxochlamys** (2)
			Parakaempferia (1)
		Tribe	*Pommereschea* (2)
		Riedelieae	*Rhynchanthus* (4)
		Burbidgea (5)	*Roscoea* (23)
		Pleuranthodium (23)	*Scaphochlamys* (34)
		Riedelia (75)	*Stadiochilus* (1)
		Siamanthus (1)	*Zingiber* (146)
		Incertae sedis	Tribe
		Siliquamomum (3)	**Globbeae**
			Gagnepainia (3)
			Globba (106)
			Hemiorchis (3)
			Incertae sedis
			Monolophus (25)

systematics (e.g., three seed characters analyzed and discussed by Grootjen and Bouman, 1981; four seed characters used in ordinal phylogenetic analyses by Kress, 1990, 1996; Kress et al., 2001).

A more recent study on seeds within subfamily Alpinioideae (Benedict et al., 2015) showed that Zingiberaceae seeds are structurally some of the most complicated seeds in angiosperms and documented 23 seed characters for the subfamily, many of which have not been used to categorize seeds prior. Benedict et al. (2015) found that Riedelieae and Alpinieae can be further distinguished based on endotesta structure and operculum layering and that many of the proposed clades of *Alpinia* sensu Kress et al. (2005, 2007) are supported by seed characters. While these studies demonstrate the usefulness of seed characters in the systematics of Alpinioideae, their utility for Zingiberaceae as a whole remains to be tested. It is the aim of this paper to (1) document novel characters not commonly described for Zingiberaceae seeds that may prove useful for future studies on angiosperm systematic and seed ecology studies within and outside of the Zingiberaceae, (2) provide details of seed morphology and anatomy of many Zingiberaceae that have not been documented previously, (3) determine whether synapomorphic characters exist for subfamilies and tribes within Zingiberaceae, and (4) determine whether seed characters can help resolve the correct placement of incertae sedis taxa within Zingiberaceae sensu Kress et al. (2002, 2005, 2007).

MATERIALS AND METHODS

Mature dried seeds of 75 taxa from three of the four subfamilies of Zingiberaceae were sampled from various herbaria, botanical gardens, or commercial growers (Table 2). The number of seeds studied per taxon ranged from one to more than 50. Each species was examined with light microscopy for external features and analyzed using synchrotron-based x-ray tomographic microscopy (SRXTM; also referred to in some literature as synchrotron radiation x-ray computed tomography, SRXCT, or SRμCT).

Light microscopy and photography—External features of the seeds were observed using a Leica MZ6 or Nikon SMZ1500 stereomicroscope and photographed using a Macropod (Macroscopic Solutions, Coventry, Connecticut, USA), outfitted with a Canon EOS 6D DSLR with a Macro Photo MP-E 65 mm manual focus lens, MT-24EX Macro Twin Light flash, and a STKS-C StackShot Macro Rail (Cognisys, Traverse City, Michigan, USA). Series of 20–75 images at various focal planes were obtained and stitched into a single image using Zerene Stacker version 1.04 software (Zerene Systems, Richland, Washington, USA). Images were edited uniformly for contrast using Adobe Photoshop CS2 (Adobe Systems, San Jose, California, USA).

Synchrotron-based x-ray tomographic microscopy—Samples were mounted onto brass stubs or toothpicks using a polyvinyl aceatate (PVA) glue or epoxy and imaged using standard absorption contrast at the TOMCAT beamline at the Swiss Light Source (SLS; Stampanoni et al., 2006; Paul Scherrer Institut, Villigen, Switzerland; specimens scanned in 2009, 2010, 2011, 2013, and 2015); the 2-BM beamline at the Advanced Photon Source (APS; Argonne National Laboratory, Lemont, Ilinois, USA; specimens scanned during sessions in 2011 and 2012); or the 8.3.2 beamline at the Advanced Light Source (ALS; MacDowell et al., 2012; Lawrence Berkeley National Laboratory, Berkeley, California, USA; specimens scanned during sessions in 2013, 2014, and 2015). Transmitted x-rays were converted into visible light using a 20 μm (SLS: 2013, 2015), 100 μm (SLS: 2013, 2015; APS), or 200 μm scintillator (SLS: 2009–2011) LAG:Ce scintillator screen (Crytur, Turnov, Czech Republic) or a 0.5 mm LuAG scintillator (Crytur; ALS).

At TOMCAT, projection data were magnified by 2×, 4×, or 20× microscope objectives and digitized by a high-resolution CCD camera (pco.2000; PCO GmbH, Kelheim, Germany; 2009–2011) or sCMOS camera (pco.edge 5.5; PCO GmbH; 2013). Samples were scanned using 10 or 13 keV and an exposure time per projection of 50, 125, 150 or 200 ms. For each scan, a total of 1501 projections (2048 × 2048 pixels with PCO.2000 camera, 2560 × 2160 pixels with PCO.edge 5.5 camera) were acquired over 180°. Reconstruction of the tomographic data were performed on a 60-node Linux PC cluster using a highly optimized routine based on the Fourier transform method and a gridding procedure (Marone et al., 2010; Marone and Stampanoni, 2012), resulting in a theoretical pixel size of 3.7 μm at 2× and 1.85 μm at 4× (2009–2011) or 3.25 μm at 2× and 1.625 μm at 4× (2013–2015) for reconstructed images.

At 2-BM, 2.5×, 4×, or 5× microscope objectives were used to magnify the projection data, and a Coolsnap K4 camera (Photometrics, Tucson, Arizona, USA; 2011 and February 2012) or pco.dimax high-speed camera (PCO GmbH, Kelheim, Germany, June 2012) was used to digitize the data. Samples were scanned at 16.1 or 21 keV with an exposure time of 280–700 ms. For each scan, a total of 1500 projections (2048 × 2048 pixels with Coolsnap K4, 2016 × 2016 for PCO) were acquired over 180°. The tomographic reconstructions were conducted with a 64-node cluster at APS using a gridrec reconstruction algorithm (Dowd et al., 1999). Reconstructed images taken with the Coolsnap K4 had a theoretical pixel size of 3.7 μm at 2×, 2.96 μm at 2.5×, 1.85 μm at 4×, and 1.48 μm at 5×, and those taken with the pco.dimax had a theoretical pixel size of 5.5 μm at 2×, 4.4 μm at 2.5×, 2.75 μm at 4××, and 2.2 μm at 5×.

At the 8.3.2 beamline, samples were magnified with either a 2× or 5× microscope objective and digitized using an sCMOS camera (pco.edge; PCO GmbH). Samples were scanned at 15 keV with an exposure time of 90, 500, or 950 ms. For each scan, a total of 2049 projections (2560 × 2160 pixels) were acquired over 180°. Reconstruction was carried out using a custom ImageJ (Rasband, 1997–2014) plug-in for image preprocessing and Octopus (Inside Matters, Aalst, Belgium) for tomographic reconstruction. Reconstructed images had a theoretical pixel size of 3.25 μm at 2× and 1.3 μm at 5×.

Reconstructed images were processed at the University of Michigan using Avizo 7.0 or 8.0 (FEI Visualization Science Group, Burlington, Massachusetts, USA) for Windows 7. Images were captured in Avizo 7.0 or 8.0 and edited uniformly for contrast using Adobe Photoshop CS2 or CS6.

Character evolution analyses—Character states that were not observable due to scanning conditions or missing data were treated as (?), and character states that were not applicable (e.g., character 14, operculum layering if no operculum was present, character 13) were treated as (–) to distinguish a lost character from a missing character in the character evolution analyses. The character matrix (Table 3) was imported into the program Mesquite v.3.03 (Maddison and Maddison, 2015), and characters were traced using parsimony onto a tree topology derived primarily from the results of the

TABLE 2. List of specimens sampled and their voucher information. Herbarium abbreviations follow Index Herbariorum (Thiers, 2015). Numbers in parentheses indicate number and type of specimens scanned per taxon.

Species	Voucher Information	Species	Voucher Information
Aframomum chrysanthum Lock	SING, GRC-173 (1 seed)	*Etlingera linguiformis* (Roxb.) R.M.Sm.	US, WJ Kress, M Bordelon, T Htum 02-7044 (1 seed)
Aframomum daniellii (Hook.f.) K.Schum.	Delft University of Technology, JW van Loon (1 seed)	*Etlingera yunnanensis* (T.L.Wu & S.J.Chen) R.M.Sm.	SING, JLS-1717 (1 seed)
Aframomum melegueta K.Schum.	US, J. Higgins 44 (1 seed)	*Gagnepainia harmandii* (Baill.) K.Schum.	SING, GRC-132 (1 seed)
Alpinia aquatica (Retz.) Roscoe	SING, GRC-22, and US, WJ Kress 05-7809 (2 seeds and 1 fruit)	*Geocharis aurantiaca* Ridl.	SING, Corner 32777 (1 seed)
Alpinia boia Seem.	US, WJ Kress 79-1071, and US, AC Smith 4087 (2 seeds)	*Geostachys densiflora* Ridl.	SING, JLS-1662 (1 seed)
Alpinia brevilabris C.Presl	US, M Ramos 30411 (1 seed)	*Globba aurea* Elmer	MICH, HH Bartlett 15543 (1 seed)
Alpinia caerulea (R.Br.) Benth.	SING, JLS-1660 (1 seed)	*Globba maculata* Blume	MICH, HH Bartlett 7544 (1 seed)
Alpinia carolinensis Koidz.	US, DH Lorence 7907 (1 seed)	*Globba pendula* Roxb.	NYBG, Rahmat Si Toroes 3668 (1 seed)
Alpinia conchigera Griff.	SING, GRC-205 (1 seed)	*Globba sessiliflora* Sims	SING, JLS-1957 (1 seed)
Alpinia fax (Thwaites) B.L.Burtt & R.M.Sm.	US, AHM Jayasuriya 1217 (1 seed and 1 fruit)	*Globba spathulata* Roxb.	US, WJ Kress 01-6914 (1 seed)
Alpinia galanga (L.) Willd.	US, Shiu Ying Hu 6225 (1 seed and 1 fruit)	*Hedychium coronarium* J.Koenig	MICH, A Shilom Tan 1771 (1 seed)
Alpinia haenkei C.Presl	US, ADE Elmer 17662 (1 seed)	*Hedychium gardnerianum* Sheppard ex Ker Gawl.	MICH, SY Smith s.n. (commercially purchased) (1 seed)
Alpinia japonica (Thunb.) Miq.	NY, Muratailcitamura 639 (1 seed)	*Hedychium hasseltii* Blume	US, T Wood 94-3700 (1 seed)
Alpinia javanica Blume	SING, Umbai and Millard 1430 (1 seed)	*Hedychium muluense* R.M.Sm.	SING, JLS-54 (1 seed)
Alpinia luteocarpa Elmer	US, Kress and Li 05-7785 (1 seed)	*Hemiorchis* sp.	US, WJ Kress 01-6884 (1 seed)
Alpinia malaccensis (Burm.f.) Roscoe	US, C Saldanha 14771 (1 seed)	*Hornstedtia conica* Ridl.	SING, SNG-35 (1 seed)
Alpinia nigra (Gaertn.) B.L.Burtt	US, WJ Kress 00-6808 (1 seed)	*Hornstedtia leonurus* (J.Koenig) Retz.	SING, SNG-174 (1 seed)
Alpinia oceanica Burkill	E, Stone and Streimann 10296 (1 seed)	*Hornstedtia scottiana* (F.Muell.) K.Schum.	US, WJ Kress 80-1129 (1 seed)
Alpinia purpurata (Vieill.) K.Schum.	E, AN Miller NGF 38482 (1 seed)	*Kaempferia pulchra* Ridl.	K, Rabil 296 (1 seed)
Alpinia rafflesiana Wall. ex Baker	SING, Ridley s.n. (1 seed)	*Monolophus sikkimensis* (King ex Baker) Veldkamp & Mood	SING, Wallich s.n. (1 seed)
Alpinia stachyodes Hance	US, n.c., 1801 (1 seed)	*Newmania* sp.	SING, JLS-1646 (1 seed)
Alpinia zerumbet (Pers.) B.L.Burtt & R.M.Sm.	US, Wen 9412, and US, Fosberg 38289 (2 seeds)	*Plagiostachys escritorii* Elmer	NY, Elmer 16216 (1 seed)
Amomum koenigii J.F.Gmel.	SING, VNM-B-1443 (1 seed)	*Plagiostachys philippinensis* Ridl.	NY, Ramos and Edaño 75626 (1 seed)
Amomum lappaceum Ridl.	SING, JLS-1667 (1 seed)	*Pleuranthodium* sp.	US, TG Hartley 10989 (1 seed)
Amomum ochreum Ridl.	SING, JLS-1670 (1 seed)	*Renealmia lucida* Maas	SING, JLS-1019 (1 seed)
Amomum sericeum Roxb.	SING, JLS-1273 (1 seed)	*Renealmia occidentalis* (Sw.) Sweet	MICH, J Vera Santos 2513 (1 seed)
Aulotandra trigonocarpa H.Perrier	K, M Bardot-Vaucoulon 1272 (1 fruit)	*Riedelia corallina* (K.Schum.) Valeton	NY, Annable 3639 (1 seed)
Boesenbergia curtisii (Baker) Schltr.	NY, Henderson 22874 (1 seed)	*Riedelia* sp.	SING, JLS-428 (1 seed)
Burbidgea stenantha Ridl.	SING, GRC-88 (1 seed)	*Roscoea alpina* Royle	AAU, 1013 (1 seed)
Camptandra ovata Ridl.	JLS-1669 (1 seed)	*Siamanthus siliquosus* K.Larsen & Mood	US, WJ Kress 99-6358 (1 seed)
Cautleya gracilis (Sm.) Dandy	MO, K-46744 (2 seeds and 1 fruit)	*Siliquamomum tonkinense* Baill.	SING, VNM-B-1469 (1 seed)
Cautleya spicata (Sm.) Baker	MICH, JC Benedict s.n. (commercially purchased) (1 seed)	*Siphonochilus aethiopicus* (Schweinf.) B.L.Burtt	MO, P Kuchar 22948 (1 seed and 1 fruit)
Curcuma montana Roxb.	SING, JLS-73474 (1 seed)	*Siphonochilus kirkii* (Hook.f.) B.L.Burtt	MO, ABKatende K1880 (2 seeds)
Curcuma pierreana Gagnep.	SING, Ly-489 (1 seed)	*Vanoverberghia sepulchrei* Merr.	NY, Ramos and Edaño 45045 (1 seed and 1 fruit)
Distichochlamys citrea M.F.Newman	SING, JLS-1615 (1 seed)	*Zingiber larsenii* Theilade	SING, JLS-1270 (1 seed)
Elettariopsis unifolia (Gagnep.) M.F.Newman	MO, JF Maxwell 00-390 (1 seed)	*Zingiber officinale* Roscoe	Delft University of Technology, JW van Loon (1 seed)
Etlingera elatior (Jack) R.M.Sm.	SING, SNG-56 (1 seed)	*Zingiber spectabile* Griff.	Delft University of Technology, JW van Loon (1 seed)
		Zingiber thorelii Gagnep.	SING, JLS-1271 (1 seed)

most recent family level study by Kress et al. (2002), which used a combined nuclear internal transcribed spacer (ITS) and plastid *trnK*/*matK* data set. The Alpinioideae portion of the phylogeny follows that of Kress et al. (2007), based on a combined ITS/*matK* data set, because it provided better resolution to the relationships of taxa within the subfamily. The placement of *Newmania* as sister to *Haniffia* was taken from Leong-Škorničková et al. (2011) , based on a combined *trnK*/*matK* and ITS data set as well, where the genus was first described and placed into a phylogenetic context within the family. The *Hedychium* clade topology was derived from Wood et al. (2000), which was based on an ITS1, ITS2, and 5.8S nuclear ribosomal DNA data set.

RESULTS

All seeds were mature, dry, and possessed seed coats derived from outer integument (testa) only; often comprising exotesta, mesotesta, and endotesta (Grootjen and Bouman, 1981; Benedict et al., 2015). Seeds were analyzed for 39 internal and external seed

TABLE 3. Distribution of seed characters and character states within Zingiberaceae. Characters and character states are as follows (see Results for descriptions of characters): (1) Natural seed color: 0, white; 1, tan/ red/ light brown; 2, dark brown/ black. (2) Seed surface: 0, striate; 1, verrucose. (3) Trichomes on seed coat or aril: 0, absent; 1, present. (4) Aril: 0, enveloping more than half of seed and tightly adpressed to the seed coat; 1, present only at micropylar end of seed, solid structure; 2, present only at micropylar end of seed, divided into many separate strands; 3, present only at micropylar end of seed, divided into few thick lobes; 4, present, enveloping more than half of the seed, but not tightly adpressed to the seed coat. (5) General seed shape: 0, ellipsoid; 1, ovoid; 2, oblate (flattened at the poles of the seed); 3, polyhedral. (6) Seeds contorted from arrangement in fruit: 0, no contortion of seeds from tight packing in fruit; 1, seed shape contorted by tight packing in fruit. (7) Seed length: 0, less than twice as long as wide; 1, at least twice as long as wide. (8) Seed body taper at micropyle: 0, absent; 1, present. (9) Seed body taper at chalaza: 0, absent; 1, present. (10) Externally visible raphe: 0, absent; 1, present. (11) External chalazal indentation: 0, absent; 1, present. (12) Micropylar region shape: 0, absent/not clearly defined; 1, conical; 2, cylindrical. (13) Operculum: 0, absent; 1, present. (14) Operculum layering; 0, more or less homogeneous; 1, multilayered. (15) Micropylar collar: 0, absent; 1, present. (16) Micropylar collar layering: 0, formed from endotesta only; 1, formed from endotesta and additional layers. (17) Thickened micropylar collar: present; 0, absent; 1, present. (18) Recurved micropylar collar: 0, weakly recurved; 1, strongly recurved. (19) Hilar rim: 0, absent; 1, present. (20) Hilar rim layering: 0, formed from exotesta; 1, formed from exotesta and mesotesta. (21) Micropylar mesotesta proliferation: 0, absent; 1, present, bulbous and wide; 2, present, cylindrical and narrow. (22) Massive chalazal testal proliferations: 0, absent; 1, present. (23) Columnar chalazal testal proliferations: 0, absent; 1, present. (24) Chalazal chamber: 0, absent; 1, *Alpinia*-type; 2, *Amomum*-type. (25) Chalazal mucro: 0, absent; 1, present. (26) Seed coat thickness: 0, 1–99 µm; 1, 100–199 µm; 2, ≥200 µm. (27) Exotesta cell type: 0, palisade; 1, more or less isodiametric or cuboidal; 2, poorly developed or destroyed in mature seed. (28) Uniform exotesta: 0, homogeneous; 1, heterogeneous; (29) Multiseriate exotesta: 0, absent; 1, present. (30) Number of types of mesotesta cells: 0, absent; 1, one type; 2, two types; 3, three types. (31) Endotesta cell shape: 0, thin parenchyma (<15 µm thickness); 1, short sclerenchyma (15–30 µm in thickness); 2, elongate sclerenchyma (≥30 µm in thickness). (32) Endotestal gap location: 0, present at the chalazal end; 1, present on the side. (33) Chalazal pigment group: 0, discoid-shaped; 1, nondiscoid-shaped. (34) Raphe canal: 0, absent; 1, present. (35) Embryo length: 0, elongate; 1, short. (36) Embryo shape: 0, straight; 1, L-shaped; 2, J-shaped. (37) Embryo base: 0, not differentiated; 1, bulbous; 2, forked. (38) Embryo–testa contact: 0, absent; 1, present. (39) Basally proliferated endosperm: 0, absent; 1, present, weak or minimal amount; 2, present, strong or copious amount. (–) character not applicable, (?) character state unknown. CI = consistency index; HI = homoplasy index; RI = retention index.

Character/ Taxon	1	2	3	4	5	6	7	8	9	10	11	12	13	14	15	16	17	18	19	20	21	22	23	24	25	26	27	28	29	30	31	32	33	34	35	36	37	38	39
CI	0.143	0.364	0.125	0.333	0.167	0.067	0.071	0.053	0.067	0.182	0.125	0.167	0.50	0.077	0.20	0.063	0.077	0.063	0.143	0.250	0.154	0.067	1.0	0.069	0.50	0.20	0.10	0.10	0.333	0.158	0.167	0.091	1.0	0.042	0.333	0.065	0.167	0.50	0.222
HI	0.857	0.636	0.875	0.667	0.833	0.933	0.929	0.947	0.933	0.818	0.875	0.833	0.50	0.923	0.80	0.938	0.923	0.938	0.857	0.750	0.846	0.933	0.0	0.931	0.50	0.80	0.90	0.90	0.667	0.842	0.833	0.909	0.0	0.958	0.667	0.935	0.833	0.50	0.778
RI	0.40	0.222	0.462	0.733	0.310	0.440	0.316	0.438	0.517	0.526	0.50	0.697	0.750	0.20	0.333	0.423	0.250	0.286	0.833	0.0	0.389	0.60	1.0	0.229	0.0	0.60	0.289	0.250	0.50	0.333	0.773	0.583	1.0	0.233	0.0	0.341	0.167	0.0	0.222
Alpinioideae																																							
Aframomum chrysanthum	2	0	0	0	0	0	0	1	1	0	0	2	1	1	1	1	0	1	1	1	1	1	0	1	0	1	0	1	0	3	1	1	1	1	0	0	0	0	2
Aframomum daniellii	2	0	0	?	0	0	0	1	1	0	0	2	1	1	1	1	0	1	1	0	1	1	0	0	0	1	0	0	0	3	1	0	1	0	0	0	1	0	2
Aframomum melegueta	2	0	0	0	0	0	0	1	1	0	0	2	1	1	1	1	0	1	1	0	1	1	0	0	0	1	0	0	0	3	1	0	1	0	0	0	1	0	2
Alpinia aquatica	2	1	0	1	2	0	0	0	0	1	1	0	1	1	1	1	1	1	0	–	0	0	0	0	0	0	2	0	0	2	1	1	1	0	0	1	0	0	2
Alpinia boia	1	0	0	0	1	0	0	1	0	0	0	0	1	1	1	0	0	1	0	–	0	1	0	2	0	1	0	1	0	2	2	1	1	1	0	1	0	1	2
Alpinia brevilabris	2	1	0	0	0	0	0	0	0	1	1	0	1	1	1	1	0	1	0	–	0	0	0	0	0	0	1	1	0	2	1	1	1	0	0	1	0	0	2
Alpinia caerulea	2	0	0	0	0	1	0	0	1	1	1	0	1	1	1	1	1	1	0	–	0	0	0	0	0	0	0	0	0	2	1	1	1	1	0	2	0	0	2
Alpinia carolinensis	2	0	0	1	1	1	0	0	1	0	0	0	1	1	1	1	1	1	0	–	0	1	0	1	0	1	0	0	0	2	1	1	1	1	0	2	0	0	2
Alpinia conchigera	2	0	0	1	2	0	0	0	0	0	0	0	1	1	1	1	1	0	0	–	0	1	0	0	0	1	0	0	0	2	2	0	1	0	1	2	1	0	2
Alpinia fax	1	0	0	0	0	0	0	0	0	0	0	0	1	1	1	0	0	1	0	–	0	1	0	1	0	1	1	0	0	3	2	1	1	1	0	2	0	0	2
Alpinia galanga	2	0	0	0	2	?	0	0	0	0	0	0	1	0	1	1	1	0	0	–	0	1	0	0	0	1	0	0	0	3	2	0	1	1	0	2	0	0	2
Alpinia haenkei	1	0	0	0	0	1	0	0	0	2	0	0	1	1	1	1	1	1	0	–	0	0	1	1	0	1	2	1	0	2	2	0	1	1	0	0	2	0	2
Alpinia japonica	?	0	0	0	0	?	0	0	0	0	0	0	1	1	1	0	0	1	0	–	0	1	0	1	0	1	2	1	0	2	2	1	1	1	0	0	2	0	2
Alpinia javanica	2	1	0	0	1	0	0	1	0	0	0	0	1	1	1	0	0	?	0	–	0	0	0	2	0	0	3	0	0	?	2	1	2	0	1	2	0	0	?
Alpinia luteocarpa	1	1	0	0	0	1	0	0	1	0	0	0	1	1	1	1	0	1	0	–	0	0	0	0	0	0	1	0	0	3	1	1	1	0	0	1	0	0	2
Alpinia malaccensis	1	1	0	0	0	1	1	0	0	2	0	0	1	1	1	1	0	0	0	–	0	1	1	2	0	1	0	0	0	2	2	0	1	1	0	0	2	0	2
Alpinia nigra	1	1	0	0	2	0	0	0	0	1	0	0	1	1	1	1	1	0	0	–	0	1	0	0	0	1	1	0	0	3	1	0	1	0	0	0	1	0	2
Alpinia oceanica	1	1	0	0	1	1	0	0	1	0	0	0	1	1	1	1	1	1	0	–	0	0	0	0	0	0	2	0	0	3	1	2	2	0	0	1	0	0	2
Alpinia purpurata	1	1	0	0	0	0	1	0	1	0	0	0	1	1	1	1	0	1	0	–	2	1	0	0	0	0	2	0	0	3	1	2	2	0	0	1	0	0	2
Alpinia rafflesiana	2	1	0	0	1	0	0	0	0	0	0	0	1	1	1	0	0	0	0	–	0	0	0	2	0	1	2	0	0	1	2	1	1	1	0	0	2	0	2

continued

TABLE 3, *continued*

Character/ Taxon	1	2	3	4	5	6	7	8	9	10	11	12	13	14	15	16	17	18	19	20	21	22	23	24	25	26	27	28	29	30	31	32	33	34	35	36	37	38	39
Alpinia stachyodes	2	0	0	0	2	0	0	0	0	1	1	0	1	1	1	1	1	0	0	–	0	1	0	0	0	1	0	0	0	3	2	0	1	1	0	2	0	0	2
Alpinia zerumbet	0	1	0	0	1	1	0	0	0	2	0	0	1	1	1	1	1	0	0	–	0	0	1	2	0	1	2	1	0	2	1	0	1	1	0	0	2	0	2
Amomum koenigii	2	0	0	0	0	0	0	1	0	0	0	0	1	1	1	0	0	1	0	–	0	1	0	0	0	2	1	0	0	2	2	1	1	0	0	0	0	0	2
Amomum lappaceum	1	1	0	0	0	1	1	0	0	0	0	0	1	1	1	0	0	1	0	–	0	1	0	0	0	1	1	0	0	2	1	1	1	0	0	0	0	0	2
Amomum ochreum	2	0	0	0	0	1	1	1	0	0	0	0	1	1	1	1	0	0	1	0	0	1	0	1	0	2	0	0	0	2	1	1	1	1	0	0	0	0	2
Amomum sericeum	2	0	0	0	1	0	0	1	1	1	0	0	1	0	1	0	0	0	0	–	0	1	0	2	0	0	0	1	0	1	2	1	1	1	0	2	0	0	2
Burbidgea stenantha	1	0	0	2	0	0	1	0	1	0	0	0	1	1	1	0	0	1	1	0	1	0	0	0	1	0	0	0	0	2	1	1	1	1	0	0	0	0	1
Elettariopsis unifolia	2	0	0	0	0	0	0	1	1	1	0	0	1	1	1	0	0	1	0	–	0	1	0	2	0	1	1	0	0	1	2	0	1	1	0	2	1	0	2
Etlingera elatior	2	0	0	0	0	0	0	1	1	1	1	0	1	0	1	0	0	0	0	–	0	0	0	0	0	0	2	0	0	0	2	0	1	0	0	1	0	0	2
Etlingera linguiformis	1	1	0	0	1	1	0	1	0	1	1	0	1	1	1	0	0	0	0	–	0	0	0	0	0	0	2	0	0	0	2	0	1	0	0	1	0	0	2
Etlingera yunnanensis	1	1	0	?	1	1	0	1	0	1	1	0	1	0	1	0	0	0	0	–	0	0	0	0	0	0	2	0	0	0	2	0	1	0	0	0	0	0	2
Geocharis aurantiaca	1	0	0	0	3	1	0	0	1	1	1	0	1	1	1	0	0	0	0	–	0	1	0	0	0	0	2	?	0	2	2	1	1	1	0	2	0	0	2
Geostachys densiflora	1	1	0	0	1	1	0	0	1	1	0	0	1	1	1	0	0	1	0	–	0	1	0	2	0	1	0	1	0	3	2	1	1	1	0	1	0	0	2
Hornstedtia conica	1	0	0	1	0	0	0	1	0	1	1	1	1	1	1	1	0	1	0	–	0	1	0	0	0	0	0	0	0	1	2	0	1	1	0	1	0	0	2
Hornstedtia leonurus	1	0	0	0	0	1	0	0	0	1	1	0	1	1	1	0	0	1	0	–	0	0	0	0	0	0	2	0	0	1	2	0	1	0	0	1	0	0	2
Hornstedtia scottiana	2	0&1	0	0	0	1	0	0	0	1	1	0	1	1	1	0	0	1	0	–	0	0	0	0	0	1	2	0	0	2	2	0	1	1	0	0	0	0	2
Plagiostachys escritorii	1	0	0	0	1	1	0	0	1	0	0	0	1	1	1	1	?	0	0	–	0	1	0	2	0	0	0	1	0	2	1	1	1	1	0	0	0	0	2
Plagiostachys philippinensis	1	0	0	0	4	1	0	0	1	0	0	0	1	1	1	0	0	1	0	–	0	1	0	2	0	0	2	1	0	2	1	1	1	1	0	0	0	0	2
Pleuranthodium sp.	2	0	0	1	2	1	0	0	0	0	1	0	1	1	1	1	1	0	0	–	0	1	0	0	0	0	0	0	0	2	1	0	1	1	0	0	0	0	2
Renealmia lucida	2	0	0	?	0	0	0	0	1	0	0	2	1	1	1	1	1	0	1	1	0	1	0	1	0	1	0	1	0	2	1	0	1	1	0	1	1	0	2
Renealmia occidentailis	1	0	0	1	1	1	0	0	1	0	0	0	1	1	1	1	1	0	1	1	0	1	0	2	0	0	0	1	0	1	1	0	1	1	0	2	0	0	2
Riedelia corallina	1	0	0	1	0	1	0	1	1	0	0	1	1	1	1	1	1	0	0	–	0	0	0	0	0	0	0	0	0	2	1	1	1	0	0	2	0	0	1
Riedelia sp.	1	0	0	1	0	0	0	1	1	0	0	1	1	0	1	1	0	1	1	1	0	0	0	0	0	0	0	0	0	1	1	1	1	0	0	1	0	0	1
Siamanthus siliquosus	2	1	1	1	1	0	0	0	1	0	0	0	1	1	1	0	0	1	0	–	0	0	0	0	0	0	0	1	0	2	1	0	1	0	0	2	0	0	2
Siliquamomum tonkinense	1&2	1	1	3	0	0	1	0	1	1	0	0	1	0	1	1	0	1	1	1	2	0	0	0	1	0	0	0	0	2	2	1	1	1	0	0	0	0	1
Vanoverberghia sepulchrei	1	0	0	0	0&1	1	0	0	1	0	0	0	1	1	1	1	0	1	0	–	0	1	0	0	0	0	0	0	0	2	1	1	1	1	0	2	0	0	2
Zingiberoideae																																							
Boesenbergia curtisii	0	0	1	?	0	0	1	0	1	0	0	2	1	0	1	0	0	1	1	1	2	1	0	2	0	0	2	0	0	2	0	0	0	0	0	2	0	0	2
Camptandra ovata	1	1	1	2	0	0	1	0	1	0	0	1	1	1	0	–	–	–	1	1	0	0	0	2	0	0	1	0	0	2	0	0	0	0	0	0	0	0	1

continued

TABLE 3, *continued*

Character/ Taxon	1	2	3	4	5	6	7	8	9	10	11	12	13	14	15	16	17	18	19	20	21	22	23	24	25	26	27	28	29	30	31	32	33	34	35	36	37	38	39
Cautleya gracilis	2	1	0	?	3	1	0	0	0	0	0	1	1	0	0	–	–	–	1	1	0	0	0	0	0	0	2	0	0	2	0	0	0	0	0	2	0	0	2
Cautleya spicata	2	1	0	?	0	0	0	0	1	0	0	2	1	0	1	0	0	1	1	1	0	0	0	2	0	0	1	0	0	2	0	0	0	1	0	2	0	0	2
Curcuma montana	1	0	0	2	0	0	1	0	1	0	0	2	1	1	1	0	0	1	1	1	1	1	0	1	0	0	0	0	0	2	0	0	0	1	0	2	0	0	2
Curcuma pierreana	1	0&1	0	2	1	0	0	1	1	0	0	1	1	1	1	0	0	1	1	1	1	1	0	0	0	0	2	0	0	2	0	0	0	1	0	1	0	0	2
Distichochlamys citrea	2	0&1	0	2	0	0	1	1	1	0	0	2	0	–	1	0	0	1	1	1	0	0	0	0	0	0	2	0	0	?	0	0	0	0	0	2	0	0	1
Gagnepainia harmandii	1	0&1	1	1	0	0	0	0	0	0	1	2	?	?	1	1	0	0	1	1	0	0	0	1	0	0	1	0	0	1	0	0	0	0	0	0	0	0	0
Globba aurea	1	0	1	1	0	1	1	1	1	0	0	1	1	1	1	1	0	1	1	1	1	1	0	2	0	0	0	0	1	2	0	0	0	1	0	1	0	0	0
Globba maculata	1	0	1	1	1	1	0	1	1	0	0	2	1	1	1	1	0	1	1	1	1	1	0	2	0	0	0	0	1	2	0	0	0	1	0	2	0	0	2
Globba pendula	1	0	1	1	1	1	0	0	1	0	0	?	1	0	1	1	0	1	1	1	1	1	0	1	0	0	1	0	1	2	0	0	0	1	0	2	0	0	2
Globba sessiliflora	1	0	1	1	1	1	0	0	1	0	0	1	1	1	1	1	0	1	1	1	1	0	0	2	0	0	1	0	1	2	0	0	0	1	0	1	0	0	2
Globba spathulata	1	0&1	1	1	1	0	1	1	1	0	0	1	1	0	0	–	–	–	1	1	0	1	0	0	0	0	1	0	0	1	0	0	0	0	0	0	0	0	2
Hedychium coronarium	1	0	0	2	1	0	0	1	1	0	0	1	0	–	1	1	1	0	1	1	0	0	0	2	0	0	0	0	0	2	0	0	0	0	0	1	0	0	2
Hedychium gardnerianum	1	1	0	2	1	0	0	1	0	0	0	1	0	–	1	1	1	1	1	1	2	0	0	2	0	0	0	0	0	2	0	1	0	1	0	1	0	0	2
Hedychium hasseltii	1	1	0	2	0	0	1	1	1	0	0	1	0	–	1	1	0	1	1	1	2	0	0	1	0	0	2	0	0	2	0	1	0	0	0	1	0	0	2
Hedychium muluense	1	0&1	0	2	0	0	1	0	1	0	0	1	0	–	1	1	0	0	1	1	2	0	0	2	0	0	1	0	0	2	0	1	0	1	0	2	0	0	1
Hemiorchis sp.	1	0&1	1	1	0	0	0	0	0	0	1	2	1	0	1	1	0	0	1	1	0	0	0	0	0	0	1	0	0	1	0	0	0	0	0	0	0	0	0
Kaempferia pulchra	1	1	0	?	1	0	0	1	0	0	1	2	1	1	1	0	0	1	1	1	2	1	0	0	0	0	2	0	0	1	0	1	1	1	0	0	1	0	?
Monolophus sikkimensis	1	1	1	?	0	0	1	1	1	0	0	1	1	1	0	–	–	–	?	?	0	0	0	0	0	0	2	0	0	1	0	0	0	0	1	0	1	0	2
Newmania sp.	2	0&1	1	2	1	0	1	1	1	0	0	2	1	0	1	0	0	1	1	1	2	1	0	2	0	0	0	0	0	2	0	1	0	1	0	2	1	0	1
Roscoea alpina	2	0&1	0	1	0	0	0	1	1	0	0	2	1	0	1	0	0	1	1	1	0	0	0	0	0	0	2	0	0	3	0	1	0	0	0	1	0	0	2
Zingiber larsenii	2	0	0	4	0	0	1	1	1	0	0	1	1	1	1	1	0	1	1	1	0	0	0	2	0	0	0	0	0	2	0	1	0	1	0	1	0	0	2
Zingiber officinale	2	1	0	?	0	0	1	1	0	0	0	1	1	1	1	1	0	1	1	1	2	0	0	0	0	0	1	0	0	2	0	1	0	0	0	1	0	0	2
Zingiber spectabile	2	0	0	4	0	0	0	1	1	0	0	1	1	1	1	1	1	1	1	1	0	0	0	1	0	0	0	0	0	2	0	1	0	1	0	1	0	0	2
Zingiber thorelii	2	0&1	0	4	0	0	1	0	1	0	0	1	1	1	1	1	0	1	1	1	2	0	0	2	0	0	0	0	0	2	0	1	0	1	0	1	0	0	2
Siphonochiloideae																																							
Aulotandra trigonocarpa	?	?	1	1	0	0	1	1	1	1?	?	1	1	1	0	–	–	–	1	1	0	0	0	0	?	0	1	0	0	?	0?	1	1	?	?	?	?	?	?
Siphonochilus aethiopicus	1	0	0	1	1	0	0	1	1	1	0	1	1	1	0	–	–	–	1	1	0	0	0	2	0	0	0	0	0	2	0	1	0	1	0	1	0	1	2
Siphonochilus kirkii	1	0	0	1	1	0	0	1	0	1	0	1	1	1	0	–	–	–	1	1	0	0	0	2	0	0	2	0	1	2	0	1	1	1	?	?	?	?	2

characters (Table 3), expanded and modified from the 23 characters identified by Benedict et al. (2015), to address the large amount of variation in Zingiberaceae seeds. Characters were determined from observations of seed external morphology and internal anatomy available from digital longitudinal and transverse sections, 3-dimensional (3D) volume renderings, and movies of serial digital longitudinal and transverse sections (between 1000–2000 sections per series). Some of the characters introduced below may be correlated, but future developmental studies are needed to determine if these correlations are developmental in nature. Digital sections and hand-colored images of digital sections of selected taxa are provided to illustrate selected seed structures discussed below (Fig. 1A–P).

Variation in seed structure—*1. Natural seed color.* Zingiberaceae seeds, when mature and dry, are often tan, red, or light brown (e.g., Fig. 2A, 2F, 2K, 2P), but can also be dark brown to black (e.g., Figs. 4A, 7F) or even white (Fig. 3A). Character states are scored as follows: 0, white; 1, tan/ red/ light brown; 2, dark brown/ black.

2. Seed surface. The surfaces of Zingiberaceae seeds can be striate (e.g., Figs. 6G, 7A, 9F), or verrucose (surfaces with small bumps, e.g., Fig. 8F). Character states are scored as follows: 0, striate; 1, verrucose.

3. Trichomes. Trichomes may (Figs. 2E, 2J, 2O, 2T, 5E, at arrows) or may not be present on the surface of the seed coat or aril. Character states are scored as follows: 0, absent; 1, present.

4. Aril. Arils and various fleshy, tubular, or disk-like appendages at the micropylar region of the seed have been given various names based on the particular region of the seed or funiculus from which they derive (Kapil et al., 1980). A detailed history and alternate classification is given by Kapil et al. (1980), in which they propose, in agreement with Corner (1976), that all aril-like structures be called arils and terms such as arilloid, arillode, false aril, and hilar aril be abandoned. They also propose that funicular arils, caruncles (derived from the exotesta, also called an exostome-aril), and strophioles (derived from the raphe tissue) be retained for descriptive purposes only. We adopt this interpretation of the definition of an aril and choose to describe arils in terms of presence and absence without making a distinction of exact origin (integumentary, funicular, or raphe tissue) due to the limited developmental understanding of many taxa within the family. While the origin of the aril is not always clear, the extent of the aril may be useful in distinguishing between taxa. Arils may be solid structures confined to the micropylar end of the seed (e.g., Figs. 2F, 7F, 7K, 9A), may consist of many separate strands (e.g., Figs. 3F, 3K, 4P) or a few thick lobes (Fig. 8A) at the micropylar end; or may envelope more than half of a seed and be tightly adpressed (e.g., Fig. 6A, 6E, 6J, 6O) or not (Fig. 3P–Q) to the seed coat. Character states are scored as follows: 0, enveloping more than half of seed and tightly adpressed to the seed coat; 1, present only at micropylar end of seed, solid structure; 2, present only at micropylar end of seed, divided into many separate strands; 3, present only at micropylar end of seed, divided into few thick lobes; 4, present, enveloping more than half of the seed, but not tightly adpressed to the seed coat.

5. and 6. Seed shape. Seeds in Zingiberaceae (and indeed across Zingiberales) vary considerably in their shape due, in part, to frequently tight packing within the fruit (J. C. Benedict and S. Y. Smith, personal observations; e.g., Figs. 2K, 7F). Therefore, seed shape was documented for those seeds located closest to the middle of each fruit, showing the least compression.

5. General seed shape. Character states are scored as follows: 0, ellipsoid; 1, ovoid; 2, oblate (flattened at the poles of the seed); 3, polyhedral.

6. Seed contorted from arrangement in fruit. Character states are scored as follows: 0, no contortion of seeds from tight packing in fruit; 1, seed shape contorted by tight packing in fruit.

7. Seed length. Seed length also varies with respect to location within the fruit and a binary character of "at least twice as long as wide" or "less than twice as long as wide" was used to generalize seed length. Character states are scored as follows: 0, less than twice as long as wide; 1, at least twice as long as wide.

8. Seed body taper at micropylar region. Character states are scored as follows: 0, absent; 1, present.

9. Seed body taper at chalazal region. In some seeds, the body has a slight decrease in width, or taper, toward the chalazal region. Character states are scored as follows:0, absent; 1, present.

10. Externally visible raphe. During maturation of the seed, the anatropous ovules of Zingiberaceae taxa may produce an externally visible groove or ridge in the seed coat corresponding to the position of the raphe in the mature seed (Figs. 8B, 9A). Character states are scored as follows: 0, absent; 1, present.

11. External chalazal indentation. As with the externally visible raphe (10), in some Zingiberaceae the chalazal region of the seed has a distinctive circular indentation, termed a "sunken chalaza" in *Costus* (Grootjen and Bouman, 1981). It is unclear whether this structure is homologous for Zingiberaceae seeds, and future developmental work is needed to understand the evolution of this trait across the order. Character states are scored as follows: 0, absent; 1, present

12. Micropylar region shape. In longitudinal section, the micropylar region, sometimes including a hilar rim, operculum, and micropylar mesotestal proliferation of cells, can range from being conical (e.g., Figs. 1A–B, 1E–H, 4B, 4G), cylindrical (e.g., Figs. 1C–D, 3B, 3R), or not clearly defined or absent. Character states are scored as follows: 0, absent/not clearly defined; 1, conical; 2, cylindrical.

13. Operculum. An operculum is found within many Zingiberaceae and is conical to disk-shaped in longitudinal section. Character states are scored as follows: 0, absent; 1, present.

14. Operculum layering. The operculum is derived from mesotesta and/or endotesta, making them either homogeneous, or formed of two (or more) distinctive layers. In SRXTM images, the inner, endotesta-derived layer often has an outer x-ray bright layer that forms a boundary with the outer mesotestal-derived layer; this

operculum, and storage tissue. (M, N) Chalazal region of *Alpinia malaccensis* with an *Alpinia*-type chalazal chamber and a columnar chalazal testal proliferation of cells. (O, P) Chalazal region of *Curcuma pierreana* with embryo, exotesta, parenchymatous endotesta, chalazal mesotestal proliferation of cells, and a discoid-shaped chalazal pigment group nested within the endotestal gap. *Abbreviations:* a, aril, light blue color; cc, chalazal chamber; cmp, chalazal mesotestal proliferation of cells; cpg, chalazal pigment group, black; eg, endotestal gap; en, parenchymatous endotesta, red; en, sclerenchymatous endotesta, light brown; em, embryo; ex, exotesta, dark brown; m, mesotesta, orange; mc, micropylar collar; mmp, micropylar mesotestal proliferation; o, operculum, outer layer light yellow, inner layer dark yellow; st, storage tissue, gray. Scale bars: 250 μm.

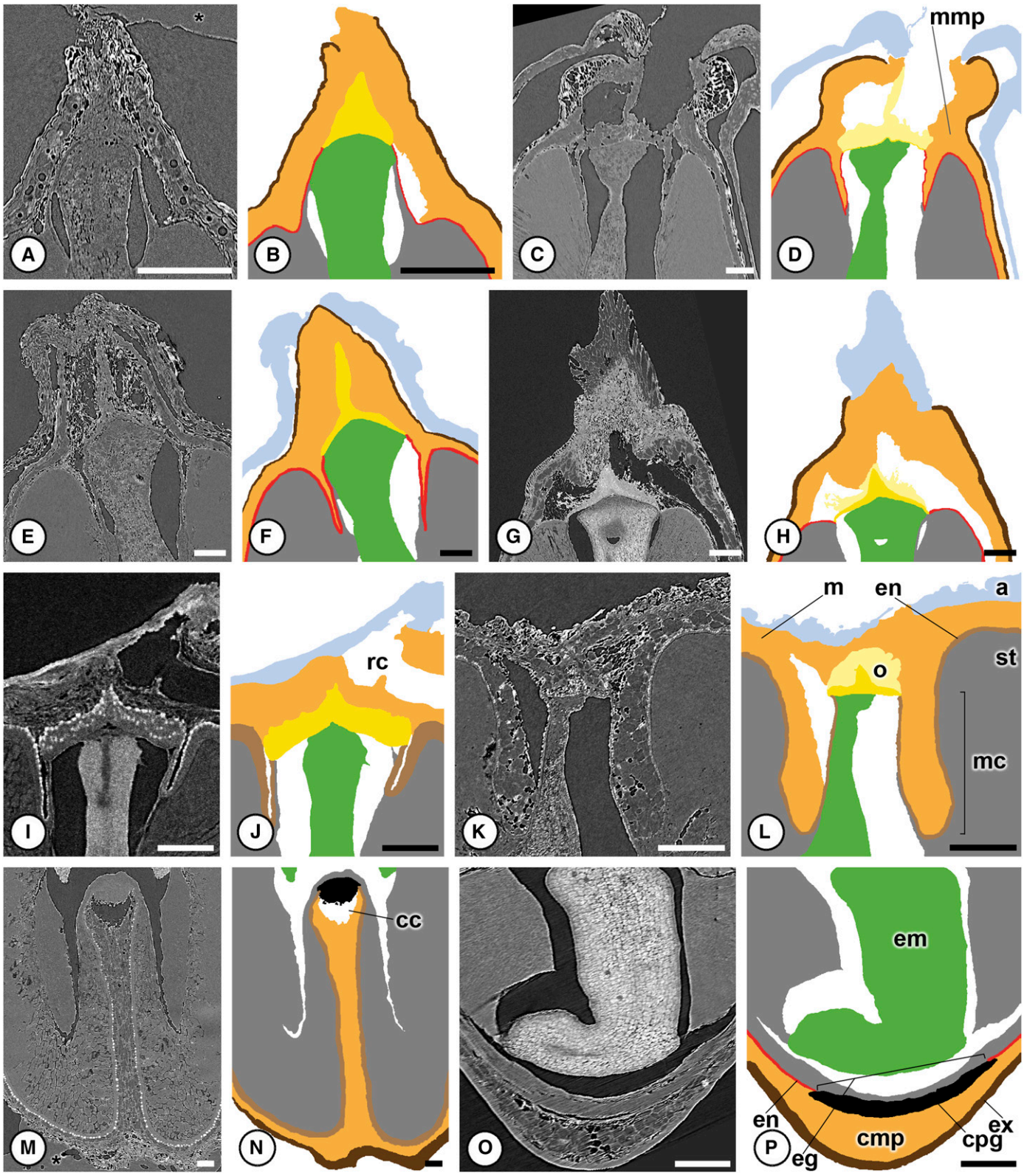

FIGURE 1 Micropylar and chalazal variation in Zingiberaceae. A, C, E, G, I, K, M, O: digital longitudinal sections; B, D, F, H, J, L, N, P: hand-colored images of digital longitudinal sections. (A, B) Conical micropylar region of *Cautleya gracilis*. (C, D) Cylindrical micropylar region with a mesotestal proliferation of cells in *Zingiber thorelii*. (E, F) Conical micropylar region of *Roscoea alpina*. (G, H) Conical micropylar region of *Siphonochilus aethiopicus*. (I, J) Micropylar region of *Elettariopsis unifolia* without a distinctive micropylar region shape. (K, L) Micropylar region of *Pleuranthodium* sp. without a distinctive micropylar region shape, an aril tightly adpressed to the seed, a micropylar collar derived from mesotesta and small sclerified endotesta, a two-layered

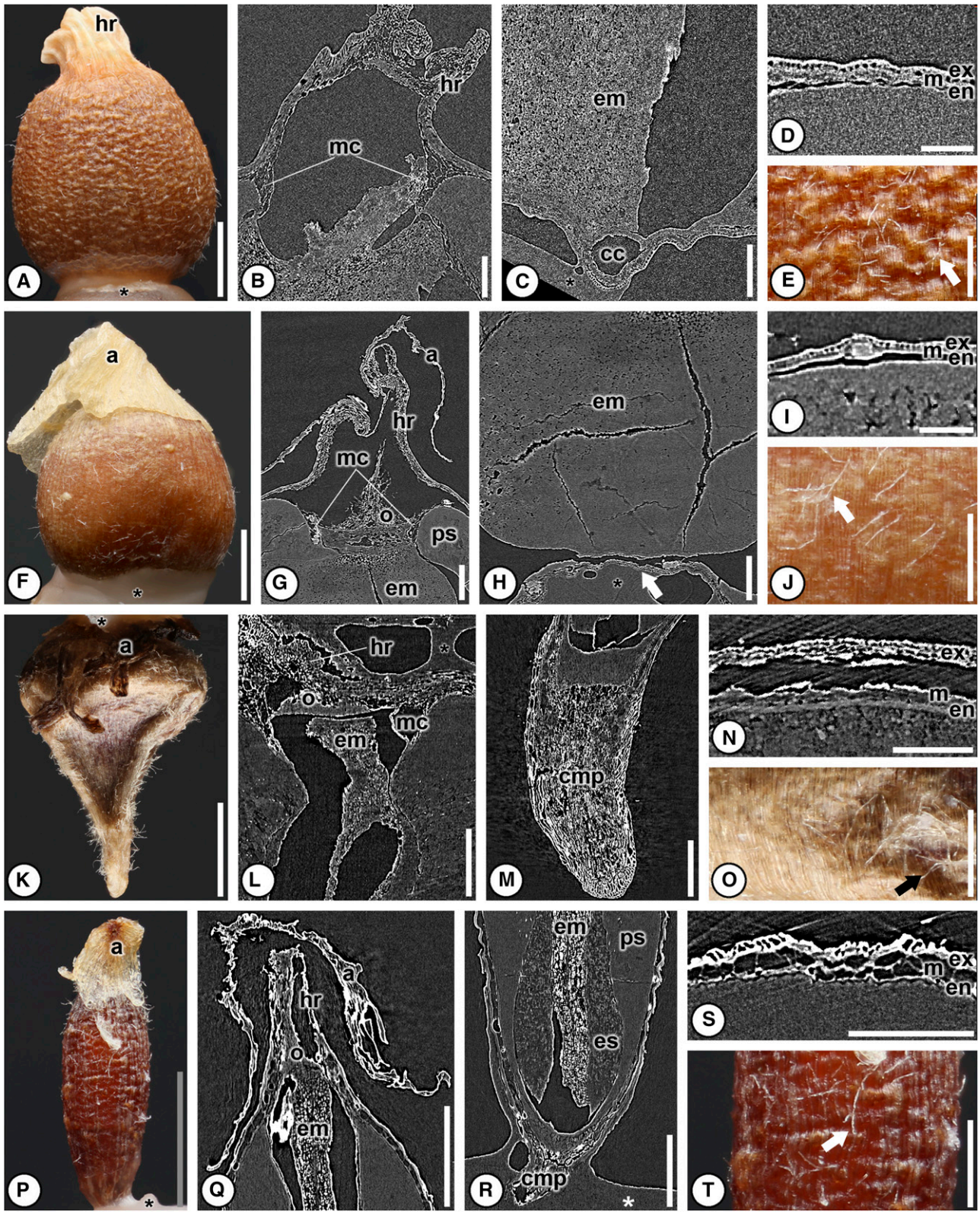

FIGURE 2 Seed anatomy in subfamily Zingiberoideae, tribe Globbeae. A, E–F, J–K, O–P, T: light micrographs; B–C, G–H, L–M, Q–R: digital longitudinal sections; D, I, N, S: digital transverse sections. (A–E) *Gagnepainia harmandii*. (A) Overview of light brown seed with hilar rim (hr) and aril detached. (B) Micropylar region showing micropylar collar (mc) and hilar rim (hr) formed of endotesta and mesotesta below aril attachment point. (C) Chalazal region with *Alpinia*-type chalazal chamber (cc) and large, basally bulbous embryo (em). (D) Testa with cuboidal exotesta (ex), single type of mesotestal cells (m), and thin endotesta (en) of parenchyma. (E) Detail of verrucose and striate seed surface with trichomes (arrow). (F–J) *Hemiorchis* sp. (F) Overview

varies from being extremely thin (Fig. 1C–D) to more substantial (Fig. 1I–J). An outer layer from mesotesta tends to be formed of larger cells, sometimes with intercellular spaces, and lacks the x-ray bright nature in SRXTM images (Fig. 1G–H, 1K–L). Character states are scored as follows: (–) no operculum present; 0, more or less homogeneous; 1, multilayered.

15. Micropylar collar. The micropylar collar (labeled "mc" in figures) is a tube or cylinder of testal cells (see character 16) that expands into the embryo chamber, often creating two "V" shapes below the operculum in longitudinal section (Fig. 1C–F, 1I–L). Some seeds appear to have shallowly or deeply infolded micropylar collars, but this character was found to be subjective in nature and thus was not included as a separate character. The apical portion of the micropylar collar is the attachment point for the operculum of many Zingiberaceae seeds and often surrounds the apical portion of the embryo (e.g., Figs. 4L, 4Q, 8D). Character states are scored as follows: 0, absent; 1, present.

16. Micropylar collar layering. The micropylar collar is formed either from the endotesta or a combination of the endotesta and mesotesta. Liao and Wu (1996) recognized three types of micropylar collars based on large-volume mesotestal cells ("form A"), small-volume mesotestal cells ("form B") or no mesotestal cells ("form C"). In our studies, the distinction of large and small mesotestal cells was found to be based on subtle differences; therefore, two are recognized here, those that are formed from mesotesta and endotesta (= forms A or B; e.g., Figs. 1C–F, 1K–L, 4L, 4Q, 7G, 7L) and those that are formed from endotesta only (= form C; e.g., Figs. 1I–J, 6K, 6P, 7B). Character states are scored as follows: (–), no micropylar collar present, therefore, character not applicable; 0, formed from endotesta only; 1, formed from endotesta and additional layers.

17. Thickened micropylar collar. The micropylar collar sometimes shows a distinctly thickened mesotesta in longitudinal section with respect to the rest of the seed coat (e.g., Figs. 1K–L, 4L, 7G, 7L). Character states are scored as follows: (–) no micropylar collar present therefore character not applicable; 0, absent; 1, present.

18. Recurved micropylar collar. The inner terminus of the micropylar collar ranges from being distinctly acute (strongly recurved, e.g., Figs. 1C–F, 7Q, 8D) to weakly recurved (e.g., Figs. 1K–L, 7G), in longitudinal section. Character states are scored as follows: (–) no micropylar collar present therefore character not applicable; 0, weakly recurved; 1, strongly recurved.

19. Hilar rim. A hilar rim (labeled "hr" in figures) is an elongated tube of seed coat that forms a rim at the micropylar region of the seed. In longitudinal section it was previously described as "[it] produces the appearance of a pair of horns arising from the hilar end of the seed" (Manchester and Kress, 1993: p. 1267; e.g., Figs. 1C–D, 2B, 2G, 3B, 7B, 8D, 10A–B). In some specimens, the rim recurves slightly inward, especially when the aril has been detached (e.g., Figs. 2G, 3B). Character states are scored as follows: 0, absent; 1, present.

20. Hilar rim layering. The hilar rim can be formed from the exotesta (e.g., Fig. 7B) or a combination of the exotesta and mesotesta (e.g., Figs. 1C–D, 3B, 4B, 5G). Character states are scored as follows: (–) no hilar rim present therefore character not applicable; 0, formed from exotesta; 1, formed from exotesta and mesotesta.

21. Micropylar mesotestal proliferation. The mesotesta of the micropylar region of the seed may have a proliferation of cells to produce a mass of cells in the shape of a donut or cylinder (labeled "mmp" in figures). In longitudinal section, this proliferation of cells is adjacent to the operculum, above and offset from the micropylar collar (e.g., Figs. 1C–D, 5L, 7B). Character states are scored as follows: 0, absent; 1, present, bulbous and wide (donut shaped; e.g., Figs. 5L, 7B); 2, present, cylindrical and narrow (e.g., 3B).

22–24. Chalazal modifications. Chalazal modifications of Zingiberaceae seeds are divided into two general forms: testal proliferations (masses of mesotestal cells that have undergone extra periclinal divisions in the chalazal region compared with the rest of the seed coat and contribute three or more rows of cells to the seed coat; characters 22 and 23) and chalazal chambers (empty cavities nested within the mesotesta of seed coats; character 24). Testal proliferations do not include raphe and chalazal pigment group cells. Two types of testal proliferations exist: (1) a simple mass of mesotestal cells (e.g., Figs. 1O, 1P, 2M, 2R, 3C, 3M, 7H; labeled "cmp" in figures), here termed massive, and (2) a wall or column of endotestal and mesotestal cells that vertically divides the lower portion of the embryo cavity into two segments, termed here a columnar mesotestal proliferation (Fig. 1M, 1N). These two chalazal modifications are not mutually exclusive, and taxa can have both a chalazal chamber and a proliferation of mesotestal cells.

22. Massive chalazal testal proliferations. Character states are scored as follows: 0, absent; 1, present.

23. Columnar chalazal testal proliferations. Character states are scored as follows: 0, absent; 1, present.

24. Chalazal chamber. Two distinct types of chalazal chambers (labeled "cc" in figures) have been identified in Zingiberaceae seeds, the *Alpinia*-type and the *Amomum*-type. The *Alpinia*-type is typically lens-shaped and less than 1/3 the width of the seed

← of light brown seed and aril (a) at micropylar end. (G) Micropylar region with aril (a), hilar rim (hr) formed from the exotesta and mesotesta, single-layered operculum (o) above embryo (em) between perisperm (ps), and micropylar collar (mc) of endotesta and mesotesta. (H) Chalazal region with a bulbous embryo (em) and a thin testa (arrow) directly above glue at the base. (I) Testa with cuboidal exotesta (ex), single type of mesotestal cells (m), and endotesta (en) of parenchyma cells. (J) Detail of striate and verrucose seed surface with trichomes (arrow). (K–O) *Globba aurea*. (K) Overview of light brown seed with dark brown aril (a) at micropylar end. (L) Micropylar region with a slightly distorted hilar rim (hr) formed from both exotesta and mesotesta, a multilayered operculum (o), a micropylar collar (mc) of endotestal and mesotestal cells, and embryo (em). (M) Chalazal region with a distinctive chalazal mesotestal proliferation (cmp). (N) Testa with a multiseriate, palisade exotesta (ex), two types of mesotestal cells (m), and an endotesta (en) of parenchyma. (O) Detail of striate seed surface covered in trichomes (arrow). (P–T) *Globba spathulata*. (P) Overview of red seed with pale yellow aril (a) at micropylar end. (Q) Micropylar region with embryo (em), hilar rim (hr) of exotesta and mesotesta, single-layered operculum (o), and no micropylar collar. (R) Chalazal region with elongate straight embryo (em), basally proliferated endosperm (es), perisperm (ps), and chalazal mesotestal proliferation of cells (cmp). (S) Testa with single-layered cuboidal exotesta (ex), a single type of mesotestal cells (m), and endotesta (en) of parenchyma cells. (T) Detail of striate and verrucose seed surface with trichomes (arrow). Scale bars: A, F, K, P = 1 mm; B–C, E, G, H, J, L–M, O, Q–R, T = 250 μm; D, I, N, S = 100 μm. * mounting glue and specimen stub.

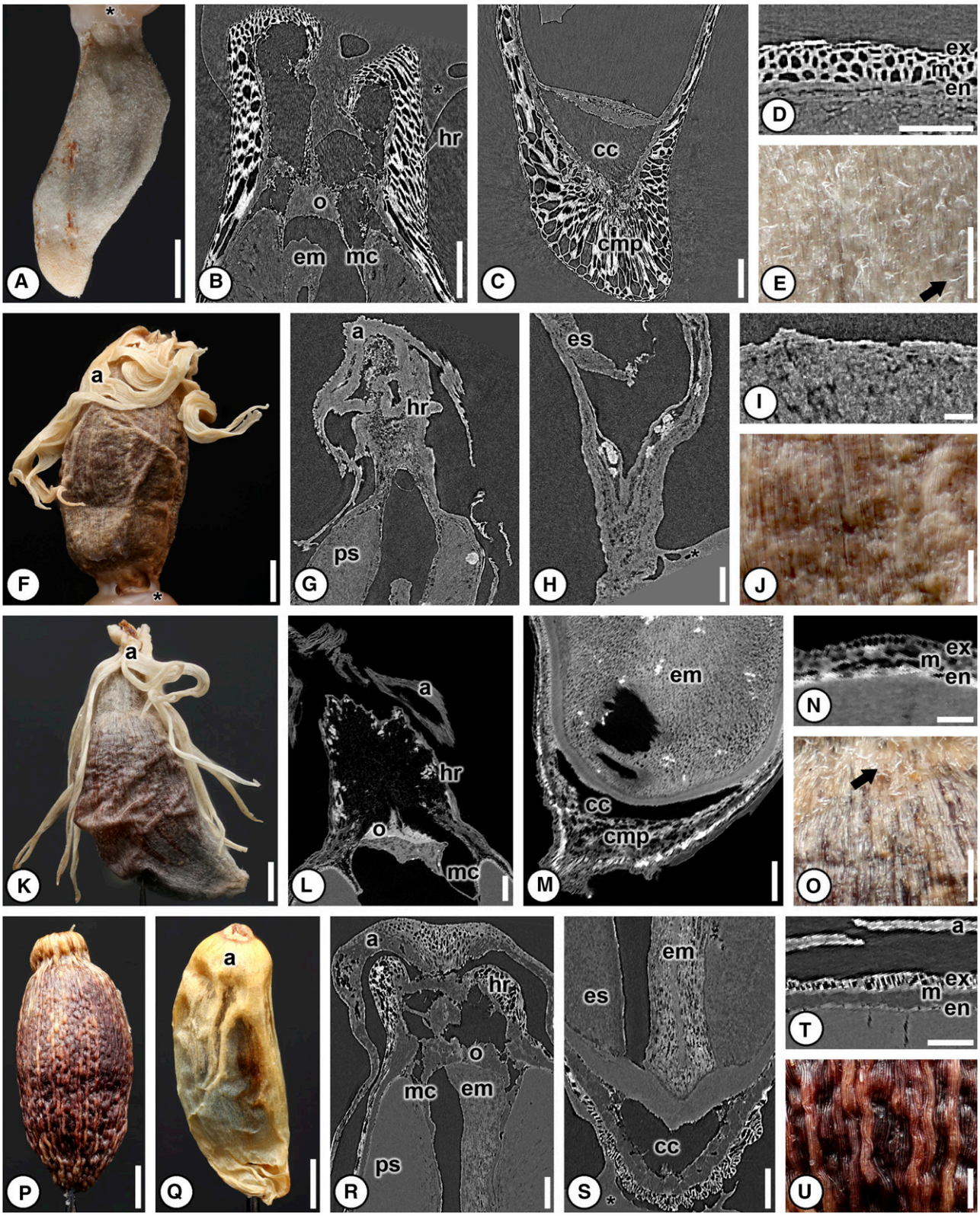

FIGURE 3 Seed anatomy in subfamily Zingiberoideae, tribe Zingibereae. A, E–F, J–K, O–Q, U: light micrographs; B–C, G, H, L–M, R–S: digital longitudinal sections; D, I, N, T: digital transverse sections. (A–E) *Boesenbergia curtisii*. (A) Overview of white seed. (B) Micropylar region with hilar rim (hr) formed from exotesta and mesotesta, single-layered operculum (o), micropylar collar (mc) formed from endotestal cells only, and embryo (em). (C) Chalazal region with *Amomum*-type chalazal chamber (cc) and chalazal mesotestal proliferation of cells (cmp). (D) Testa with poorly developed exotesta (ex), thick-walled mesotestal cells (m), both of which contribute to the white seed color, and endotesta of thin parenchyma (en). (E) Detail of white seed

(e.g., Figs. 1M, 1N, 5H, 9E), whereas the *Amomum*-type is more than 1/3 the width of the seed and often connects to (and becomes continuous with) the raphe canal in the seed (e.g., Figs. 3C, 6B, 6F). Character states are scored as follows: 0, absent; 1, *Alpinia*-type; 2, *Amomum*-type.

25. Chalazal mucro. A chalazal mucro (labeled "cm" in figures)—an abrupt, pointed termination of the seed (in contrast to character 9, which is a gradual tapering of the seed body)—was reported by Ridley (1909) who suggested the structure (termed "terminal mucro") was a modification for water and wind dispersal in *Burbidgea*. It has since also been found in other Alpinioideae as well (Benedict et al., 2015). The structure is composed of endotesta, mesotesta, and exotesta (Figs. 7A, 7C, 8E). Character states are scored as follows: 0, absent; 1, present.

26. Seed coat thickness. The seed coat (all layers of the testa) thickness is determined in transverse sections in the middle of the seed and is measured at the thinnest region of the seed coat. Character states are scored as follows: 0, 1–99 μm; 1, 100–199 μm; 2, ≥200 μm.

27. Exotesta cell type. The exotesta can be made of palisade cells (e.g., Fig. 7D, 7I), generally isodiametric cells (e.g., Fig. 6H), be poorly developed (e.g., 3D), or it can be absent. Character states are scored as follows: 0, palisade; 1, more or less isodiametric or cuboidal; 2, poorly developed or destroyed in mature seed.

28. Uniform exotesta. The exotesta is most commonly composed of a homogeneous layer of cells, but it can also be heterogeneous with cells that vary in shape as a result of irregular anticlinal divisions of the exotesta (e.g., Figs. 2S, 3T). Character states are scored as follows: 0, homogeneous; 1, heterogeneous.

29. Multiseriate exotesta. Previously described as a multiple epidermis by some authors (e.g., Wu and Liao, 1995; Liao and Wu, 2000), the exotesta is often uniseriate, but can be multiseriate with two or more cell layers (e.g., Fig. 2N). Character states are scored as follows: 0, absent; 1, present.

30. Number of types of mesotestal cells. The mesotesta, when differentiated, is composed of three cell types occurring in distinct layers in Zingiberaceae seeds (Liao and Wu, 1996, 2000). These layers have been previously described as the hypodermis (directly beneath the exotesta), the translucent cell layer (beneath the hypodermis) and the pigment layer (beneath the translucent cell layer and above the endotesta). In some taxa, the three types can be discerned (e.g., Fig. 4I), whereas in others it is either absent, a single type (e.g., Fig. 6D, 6H), or two types (e.g., Figs. 4S, 9G). Character states are scored as follows: 0, absent; 1, one type; 2, two types; 3, three types.

31. Endotestal cell thickness and shape. The endotesta is the innermost layer of cells of the seed coat in Zingiberaceae seeds. Its thickness and shape vary considerably and can range from very small square to rectangular sclerified cells that are less than 30 μm in thickness (e.g., Fig. 6N), to palisade sclerified cells 30 μm or greater in thickness (e.g., Fig. 6D, 6H), to a thin layer, <15 μm, of parenchyma cells (e.g., Figs. 2N, 2S, 3T). Character states are scored as follows: 0, thin parenchyma (<15 μm thickness); 1, short sclerenchyma (15–30 μm in thickness); 2, elongate sclerenchyma (≥30 μm in thickness).

32. Endotestal gap location. The endotesta has a small circular to ellipsoid interruption, often in the chalazal region of seed, and typically represents the point where the raphe terminates in the seed coat. In longitudinal section, this endotestal gap is filled by the chalazal pigment group so is not seen as a true void (e.g., Figs. 1M–P, 6L, 6Q). The location of the gap varies from being at the base of the seed (Fig. 6Q) to the side of the seed (Fig. 7R). Character states are scored as follows: 0, present at the chalazal end; 1, present on the side.

33. Chalazal pigment group. As noted in previous studies (Liao and Wu, 1996, 2000), the chalazal pigment group (cpg) is a small collection of cells in the embryo cavity above the raphe and endotestal gap. Previously, it was determined that members of Zingiberoideae have a discoid-shaped cpg, termed crescent-shaped by Liao and Wu (2000; Figs. 1O–P, 5M), while members of Alpinioideae have "trumpet-shaped" cpgs (Liao and Wu, 2000) or otherwise nondiscoid cpgs (Figs. 1M–N, 6L). Character states are scored as follows: 0, discoid-shaped; 1, nondiscoid-shaped.

34. Raphe canal. The raphe in mature seeds is destroyed on some taxa, leaving a canal in the seed coat from the micropyle to the chalaza (Fig. 6F; labeled "rc" in figures). In some specimens the raphe canal terminates at (and merges with) the chalazal chamber (e.g., Fig. 6F), but can be differentiated from the chalazal chamber by being slightly smaller in diameter. Character states are scored as follows: 0, absent; 1, present.

35. Embryo length. The embryos in most Zingiberaceae are elongate and extend for more than half the length of the seed, but in some taxa they are much shorter. Character states are scored as follows: 0, elongate; 1, short.

36. Embryo shape. The shape of the embryo ranges from being straight (Fig. 8C), L-shaped (with a sharp, nearly right-angled curve in the embryo that is less than 25% of the embryo length, Fig. 9B), to J-shaped (with a smooth curve in the embryo that is ca. 50% of the embryo length, Fig. 6F). Character states are scored as follows: 0, straight; 1, L-shaped; 2, J-shaped.

←

surface covered in trichomes (arrow). (F–J) *Distichochlamys citrea.* (F) Overview of dark brown seed with aril (a) of several strands. (G) Micropylar region with hilar rim (hr) formed from endotestal and mesotestal cells subtending arillate tissue (a), perisperm (ps), and lacking operculum. (H) Chalazal region with abundant, basally proliferated endosperm (es). (I) Poorly differentiated seed coat. (J) Detail of striate and verrucose seed surface. (K–O) *Newmania* sp. (K) Overview of dark brown seed with aril (a) of several strands. (L) Micropylar region with aril (a), hilar rim (hr) of mesotestal and exotestal cells, and single-layered operculum (o) above micropylar collar (mc) formed from endotestal cells. (M) Chalazal region of seed showing enlarged, basally bulbous embryo (em), *Amomum*-type chalazal chamber (cc), and chalazal mesotestal proliferation (cmp). (N) Testa with palisade exotesta (ex), two types of mesotestal cells (m), and endotesta of parenchyma (en). (O) Detail of striate and verrucose seed surface with trichomes (arrow). (P–U) *Zingiber thorelii*. (P) Overview of seed with aril removed. (Q) Overview of seed with enveloping aril (a) not tightly adpressed to the seed coat. (R) Micropylar region with large aril (a), hilar rim (hr) of endotesta and mesotesta, a two-layered operculum (o), micropylar collar (mc) formed from both endotesta and mesotesta, perisperm (ps), and embryo (em). (S) Chalazal region with *Amomum*-type chalazal chamber (cc), elongated embryo (em), and abundant, basally proliferated endosperm (es). (T) Aril (a) and testa with palisade exotesta (ex), two types of mesotestal cells (m), and endotesta (en) of parenchyma cells. (U) Detail of verrucose, striate seed surface. Scale bars: A, F, K, P, Q = 1 mm; B–C, E, G–H, J, L–M, O, R–S, U = 250 μm; D, I, N, T =100 μm. * mounting glue and specimen stub.

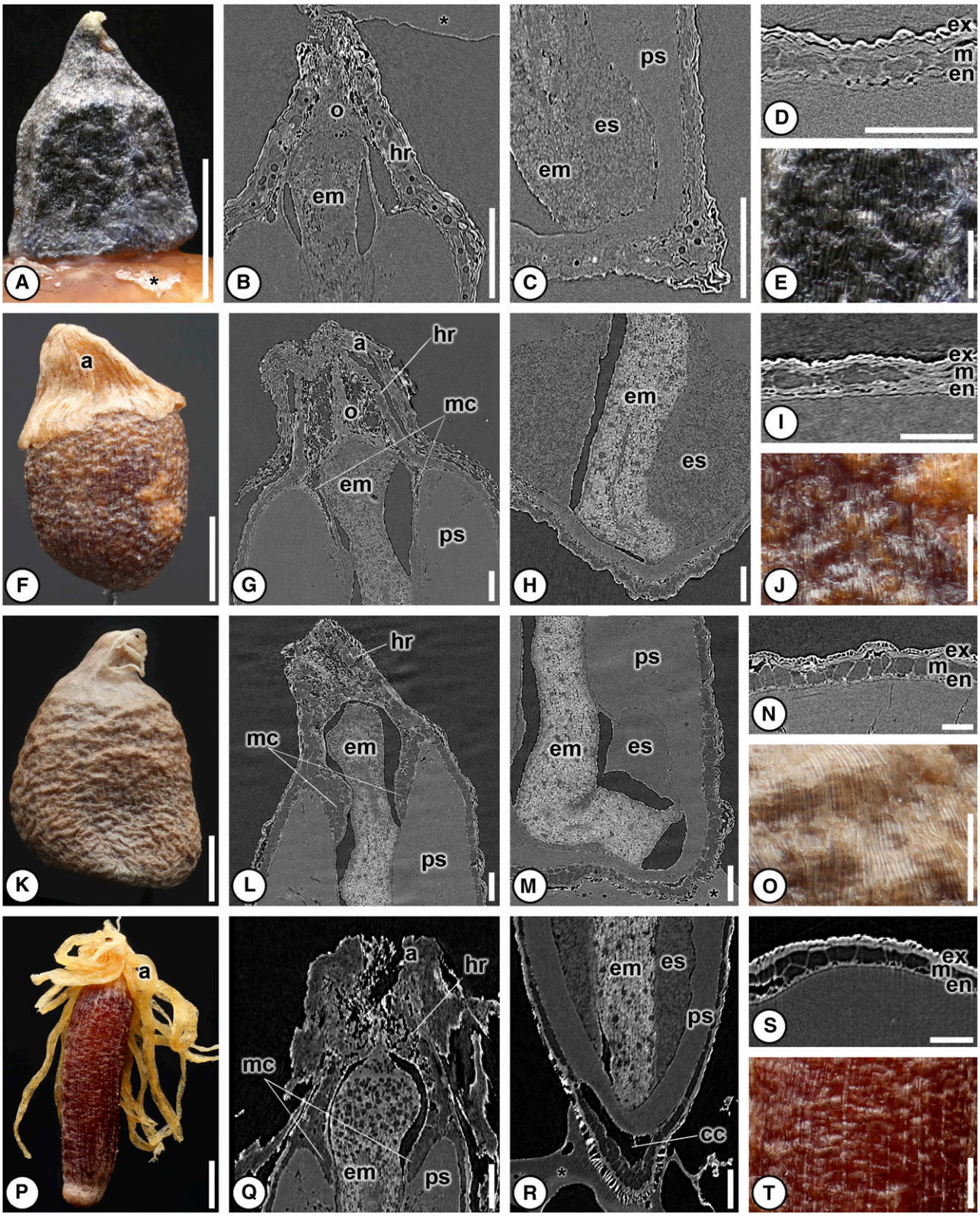

FIGURE 4 Seed anatomy of subfamily Zingiberoideae, tribe Zingibereae, part I. A, E–F, J–K, O–P, T: light micrographs; B–C, G–H, L–M, Q–R: digital longitudinal sections; D, I, N, S: digital transverse sections. (A–E) *Cautleya gracilis*. (A) Overview of black seed with aril removed. (B) Micropylar region with single-layered operculum (o), hilar rim (hr) of endotestal and mesotestal cells, embryo (em), and no micropylar collar. (C) Chalazal region with embryo (em), abundant, basally proliferated endosperm (es), and perisperm (ps). (D) Testa with a poorly developed exotesta (ex), two types of mesotestal cells (m), and endotesta (en) of parenchyma cells. (E) Detail of striate, verrucose seed surface. (F–J) *Roscoea alpina*. (F) Overview of dark brown seed with

37. Embryo base. Independent of shape, some taxa have embryos that are enlarged (bulbous; e.g., Figs. 3M, 5Q) or forked (e.g., Fig. 6B) at the base. Character states are scored as follows: 0, not differentiated; 1, bulbous; 2, forked.

38. Embryo–testa contact. The embryo, perisperm, and sometimes endosperm occupy the embryo cavity of Zingiberaceae seeds. The embryo can either be in direct contact with the seed coat (Figs. 9E) or nested within endosperm/perisperm and not touching the innermost wall of the seed coat. Character states are scored as follows: 0, absent; 1, present.

39. Basally proliferated endosperm. Endosperm in some taxa is found in greater abundance surrounding the base of the embryo (e.g., Figs. 3S, 4M, 6F) compared with the micropylar end. In some SRXTM images, the perisperm is often composed of large cells (e.g., Fig. 5C), and endosperm is often darker and lacks observable cell walls (e.g., Fig. 6F). In other SRXTM images, the endosperm appears as small cells (perhaps nuclei; e.g., Fig. 5R), and individual perisperm cells are indistinguishable (e.g., Fig. 5R). In both cases, endosperm always immediately surrounds the embryo, and both the embryo and endosperm are nested within the perisperm (e.g., Figs. 2R, 5C, 7H, 9C). This character refers to the relative distribution of endosperm and whether it is proliferated, or more abundant, toward the chalazal end of the seed as compared with the micropylar end. Character states are scored as follows: 0, absent; 1, present, weak or minimal amount; 2, present, strong or copious amount.

Zingiberaceae seeds in a systematic context—Results for all species studied are summarized in Table 3. All tribes of Alpinioideae and Zingiberoideae were sampled as well as the subfamily Siphonochiloideae, which was previously unknown for seed morphoanatomy. It was not possible to study the monospecific subfamily Tamijioideae as no herbarium we contacted (E, K, MO, MICH, NY, SING, US) had fruit or seed material available.

Zingiberoideae—Fourteen genera and 26 species representing both tribes were examined (Figs. 1A–F, 1O–P, 2A–T, 3A–U, 4A–T, 5A–T). The seeds of the 26 species studied from Zingiberoideae have in common 10 character states (character numbers in parentheses). They all lack an externally visible raphe (10), have no columnar chalazal testal proliferation of cells (23), no chalazal mucro (25), and their embryos are nested within nutrient tissue and do not contact the endotesta (38). All Zingiberoideae seeds have seed coats less than 100 μm in thickness (26; Figs. 2D, 2I, 2N, 2S, 3D, 3I, 3N, 3T, 4D, 4I, 4N, 4S, 5D, 5I, 5N, 5S), a hilar rim formed from exotestal and endotestal layers (19 and 20; Figs. 2B, 2G, 2L, 2Q, 3B, 3G, 3L, 3R, 4B, 4G, 4L, 4Q, 5B, 5G, 5L), a thin endotesta of parenchyma (31; Figs. 2D, 2I, 2N, 2S, 3D, 3I, 3N, 3T, 4D, 4I, 4N, 4S, 5D, 5I, 5N, 5S), an endotestal gap at the base of the seed (32; e.g., Fig. 1O–P), and a discoid chalazal pigment group (33; Figs. 1O–P, 5M).

The seven species of all three genera within Globbeae (Fig. 2A–T) have in common 16 characters. All seeds are lightly pigmented (tan, red, or light brown) (1; Fig. 2A, 2F, 2K, 2P), have trichomes on either the surface of the seed or aril (3; Fig. 2E, 2J, 2O, 2T), an aril confined to the micropylar end of the seed that is a solid structure (4; Fig. 2F, 2K, 2P), a hilar rim formed from both the exotesta and mesotesta (19 and 20; Fig. 2B, 2G, 2L, 2Q), seed coats less than 100 μm thick (26; Fig. 2D, 2I, 2N, 2S), a thin parenchymatous endotesta (31; Fig. 2D, 2I, 2N, 2S), an endotestal gap at the base of the seed (32), a discoid-shaped chalazal pigment group (33), and elongate embryos that are not differentiated at the base and do not touch the endotesta (35, 37, 38; Fig. 2C, 2H, 2R). They all lack an externally visible raphe (10), a columnar chalazal testal proliferation of cells (23), a chalazal mucro (25), and a uniform exotesta (28; Fig. 2D. 2I, 2N, 2S). A micropylar collar (15) was found in all taxa except *Globba spathulata* Roxb. (Fig. 2Q). The combination of a weakly recurved micropylar collar (19; Fig. 2B, 2G), the absence of basally proliferated endosperm (39; Fig. 2C, 2H), and the presence of an external chalazal indentation (11) were found to unite *Hemiorchis* sp. and *Gagnepainia harmandii* (Baill.) K.Schum. and differentiate these two genera from *Globba*.

Ten genera and 18 species were analyzed within the tribe Zingibereae (Figs. 3A–U, 4A–T, 5A–T) and found to have 13 characters in common. Seeds all have a hilar rim formed from the exotesta and mesotesta (19 and 20; Figs. 3B, 3R, 4Q), seed coats less than 100 μm in thickness (26; Figs. 3D, 3I, 3N, 3T, 4D, 4I, 4N, 4S, 5D, 5I, 5N, 5S), a thin parenchymatous endotesta (31), an endotestal gap at the base of the seed (32; Figs. 1O–P, 5M), a discoid chalazal pigment group (33; Fig. 5M), and an elongate embryo that does not contact the endotesta (35 and 38; Figs. 3M, 3S, 4H, 4M, 4R, 5M). They lack an externally visible raphe (10), columnar chalazal testal proliferations (23), a chalazal mucro (25), and a uniform or multiseriate exotesta (28 and 29). A bulbous embryo base (37) was found in *Newmania* (Fig. 3M) only, and a micropylar collar (15) was found in all but two species, *Camptandra ovata* Ridl. (Fig. 5B) and *Cautleya gracilis* (Sm.) Dandy (Fig. 4B). The shape of the seed (5) and the embryo (36), as well as the type of cells in the exotesta (27), were all found

←

solid aril (a) at micropylar end. (G) Micropylar region with aril (a), multilayered operculum (o) above embryo (em) and perisperm (ps), hilar rim (hr), and micropylar collar (mc) of endotestal cells only. (H) Chalazal region with L-shaped embryo (em) and abundant, basally proliferated endosperm (es). (I) Testa showing poorly developed exotesta (ex), three types of mesotestal cells (m), and endotesta (en) of parenchyma. (J) Detail of verrucose and striate seed surface. (K–O) *Hedychium gardnerianum*. (K) Overview of light brown seed without aril. (L) Micropylar region with thickened micropylar collar (mc) formed from endotesta and mesotesta, a hilar rim (hr), embryo (em) perisperm (ps), and no operculum. (M) Chalazal region with L-shaped embryo (em), abundant, basally proliferated endosperm (es), and perisperm (ps). (N) Testa with palisade exotesta (ex), two types of mesotestal cells (m), and endotesta of parenchyma (en). (O) Detail of striate, verrucose seed surface. (P–T) *Hedychium muluense*. (P) Overview of red seed with aril (a) divided into many thin strands. (Q) Micropylar region with aril (a), embryo (em), perisperm (ps), hilar rim (hr) and micropylar collar (mc), both formed from of both endotesta and mesotesta. (R) Chalazal region with *Amomum*-type chalazal chamber (cc), embryo (em), perisperm (ps), and abundant, basally proliferated endosperm (es). (S) Testa with isodiametric exotesta (ex), two types of mesotestal cells (m), and endotesta (en) of parenchyma cells. (T) Detail of striate, verrucose seed surface. Scale bars: A, F, K, P = 1 mm; B–C, E, G–H, J, L–M, O, Q–R, T = 250 μm; D, I, N, S = 100 μm. * mounting glue and specimen stub.

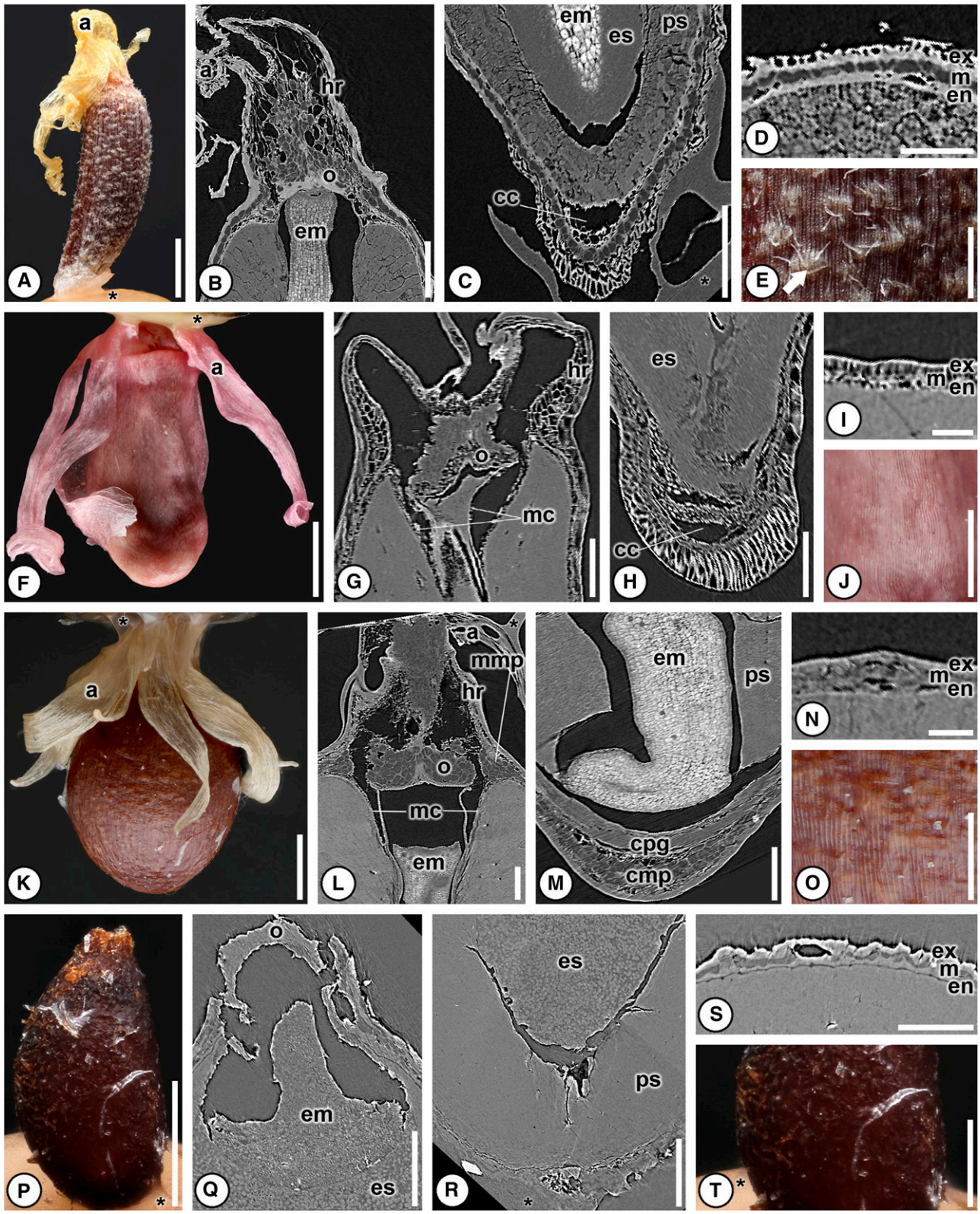

FIGURE 5 Seed anatomy of subfamily Zingiberoideae, tribe Zingibereae, part II. A, E–F, J–K, O–P, T: light micrographs; B–C, G–H, L–M, Q–R: digital longitudinal sections; D, I, N, S: digital transverse sections. (A–E) *Camptandra ovata*. (A) Overview of red seed with aril (a) divided into thin strands. (B) Micropylar region with aril (a), multilayered operculum (o), hilar rim (hr) of exotesta and mesotesta, embryo (em), and no micropylar collar. (C) Chalazal region with *Amomum*-type chalazal chamber (cc), straight embryo (em), perisperm (ps), and abundant, basally proliferated endosperm (es). (D) Testa with cuboidal exotesta (ex), two types of mesotestal cells (m), and endotesta (en) of parenchyma. (E) Detail of verrucose seed surface

to be quite variable in the tribe and not useful in distinguishing the tribe from other Zingiberaceae.

The seeds of *Monolophus sikkimensis* (King ex Baker) Veldkamp & Mood are the smallest described for Zingiberaceae (1.1 mm long × 0.6 mm wide) and can be distinguished from all other Zingiberaceae by the absence of a micropylar collar (15; Fig. 5Q), presence of a short, straight, bulbous embryo (35–37; Fig. 5Q), and having basally proliferated endosperm that fills more than half of the embryo cavity (39; Fig. 5R).

Alpinioideae—Sixteen genera and 46 species were examined from Alpinioideae (Figs. 6A–S, 7A–T, 8A–G), representing both tribes. Two characters are shared among all alpinioid taxa: lack of a multiseriate exotesta (29; Figs. 6D, 6H, 6N, 6S, 7D, 7I, 7N, 7S, 8G), and the presence of a nondiscoid chalazal pigment group (33; e.g., Figs. 1M–N, 6L, 6Q, 7H).

Eleven genera and 40 species from the tribe Alpinieae (Fig. 6A–S) were analyzed. Seven characters were found in common. All seeds of Alpinieae lack trichomes (3; Fig. 6C, 6G, 6M, 6R), have an operculum (13; Fig. 6B, 6F, 6I, 6K, 6P), have a micropylar collar (15; Fig. 6I, 6K, 6P), lack a chalazal mucro (25; Fig. 6A, 6E, 6J, 6O), and lack a multiseriate exotesta (29; Fig. 6D, 6H, 6N, 6S). Characters that were present in all Alpinieae studied were a nondiscoid chalazal pigment group (33; Figs. 1M–N, 6L, 6Q), and basally proliferated endosperm (39; Fig. 6F, 6Q). A hilar rim (19) was lacking in all Alpinieae except *Aframomum* species. *Alpinia boia* Seem. was the only taxon observed to have an embryo in contact with the endotesta (38). Both the presence and type of aril (4) and the shape of the embryo (36) were quite variable within the tribe and not useful for distinguishing the tribe from other Zingiberaceae.

The five species of Riedelieae (Fig. 7A–T) that were analyzed had 12 seed characters in common. All seeds of Riedelieae lacked an externally visible raphe (10), a columnar chalazal chamber (23), a chalazal chamber (24), and a multiseriate exotesta (29). They all shared the presence of an operculum (13; Fig. 7B, 7G, 7L, 7Q), the presence of a micropylar collar (15; Fig. 7B, 7G, 7L, 7Q), seed coats less than 100 µm thick (26; Fig. 7D, 7I, 7N, 7S), an exotesta of isodiametric or cuboidal cells (27; Fig. 7D, 7I, 7N, 7S), a nondiscoid chalazal pigment group (33; Fig. 7H, 7R), an elongated embryo (35; Fig. 7M, 7R), an embryo that is not modified at the base (37; Fig. 7H, 7M, 7R), and an embryo that does not touch the endotesta (38; Fig. 7H, 7M, 7R).

Many other characters were present in most, but not all, of the Riedelieae and thus are potentially useful for narrower taxonomic groups but are not useful for identifying the tribe. Generally the tribe had striate seeds (2), lacked trichomes (3), and had a uniform exotesta (28), but in *Siamanthus siliquosus* K.Larsen & Mood, verrucose seeds with trichomes (3) and a nonuniform exotesta (28) were observed (Fig. 7P, 7S–T). In *Burbidgea stenantha* Ridl. (Fig. 7A–E), elongate seeds (7), with a few-stranded aril (4), and chalazal mucro (25), were observed in contrast to relatively short seeds, with a solid aril, and no chalazal mucro as seen in the other members of Riedelieae. *Riedelia* sp. was found to have a homogeneous operculum (14), and a single type of mesotestal cells (30), counter to the heterogeneous opercula and a mesotesta of two distinct cell types observed in all other members of the tribe. The combination of a verrucose seed surface (2), presence of trichomes (3), and a nonuniform exotesta (28) was unique to *Siamanthus siliquosus* (Fig. 7P–T). A few stranded aril (4), elongate seed (7), and chalazal mucro (25) in combination were found only in *Burbidgea stenantha*. The seed of *Pleuranthodium* sp. (Fig. 7F–J) did not significantly taper at the chalaza (9), but had an external chalazal indentation (11) and a chalazal proliferation of cells (22) resulting in a suite of character states that differed from all other Riedelieae studied.

The large and elongate seeds of *Siliquamomum tonkinense* Baill. (Fig. 8A–G) can be easily distinguished from other Zingiberaceae by the presence of an aril confined to the micropylar region of the seed that is separated into two or three thick strands (4; Fig. 8A), conspicuous trichomes on the aril and seed coat (3; Fig. 8A, 8F), a single externally visible raphe (10; Fig. 8B), and a distinctive chalazal mucro at the base of the seed (25; Fig. 8C, 8E).

Finally, three characters in particular were found to have considerable variation within the Riedelieae: the overall shape of the seed (5), and the thickness (17), and recurvature (18) of the micropylar collar.

Siphonochiloideae—Two genera and three species were analyzed for Siphonochiloideae (Fig. 9A–G). They can be distinguished from all other Zingiberaceae by a combination of characters that includes a solid aril confined to the micropyle of the seed (4; Fig. 9A, 9D), the absence of a micropylar collar (15; Fig. 9D), and the presence of a distinct externally visible raphe from the micropyle to the chalaza of the seed (10; Fig. 9A).

DISCUSSION

The complexity of key aspects of the Zingiberaceae seeds (notably in micropylar, hilar, and chalazal regions; but also in presence of

covered in clusters of trichomes (arrow). (F–J) *Curcuma montana*. (F) Overview of seed with aril (a) divided into thin strands. Note: pink color of seed results from aceto-orcein stain and not natural pigment. (G) Micropylar region of seed with hilar rim (hr) of exotesta and mesotesta, multilayered operculum (o), and micropylar collar (mc) of endotesta only. (H) Chalazal region with *Alpinia*-type chalazal chamber (cc) and abundant, basally proliferated endosperm (es). (I) Testa with palisade exotesta (ex), two types of mesotestal cells (m), and thin endotesta of parenchyma (en). (J) Detail of striate seed surface. (K–O) *Curcuma pierreana*. (K) Overview of light brown seed coat and aril (a) divided into many strands. (L) Micropylar region with aril (a), hilar rim (hr) of exotesta and mesotesta, bulbous and wide micropylar mesotestal proliferation of cells (mmp), multilayered operculum (o), and micropylar collar (mc) formed from endotesta only. (M) Chalazal region with L-shaped embryo (em), perisperm (ps), discoid-shaped chalazal pigment group (cpg), and chalazal mesotestal proliferation (cmp). (N) Testa showing poorly developed exotesta (ex), two types of mesotestal cells (m), and endotesta (en) of parenchyma. (O) Detail of striate and verrucose seed surface. (P–T) *Monolophus sikkimensis*. (P) Overview of red seed. (Q) Micropylar region with operculum (o), bulbous short embryo (em), and abundant, basally proliferated endosperm (es). (R) Chalazal region with endosperm (es) and perisperm (ps). (S) Testa showing poorly developed exotesta (ex), single type of mesotestal cells (m), and thin, parenchymatous endotesta (en). (T) Detail of seed surface. Scale bars: A, F, K = 1 mm; P = 500 µm; B–C, E, G–H, J, L–M, O, T = 250 µm; D, I, N, Q, R = 100 µm; S = 50 µm. * mounting glue and specimen stub.

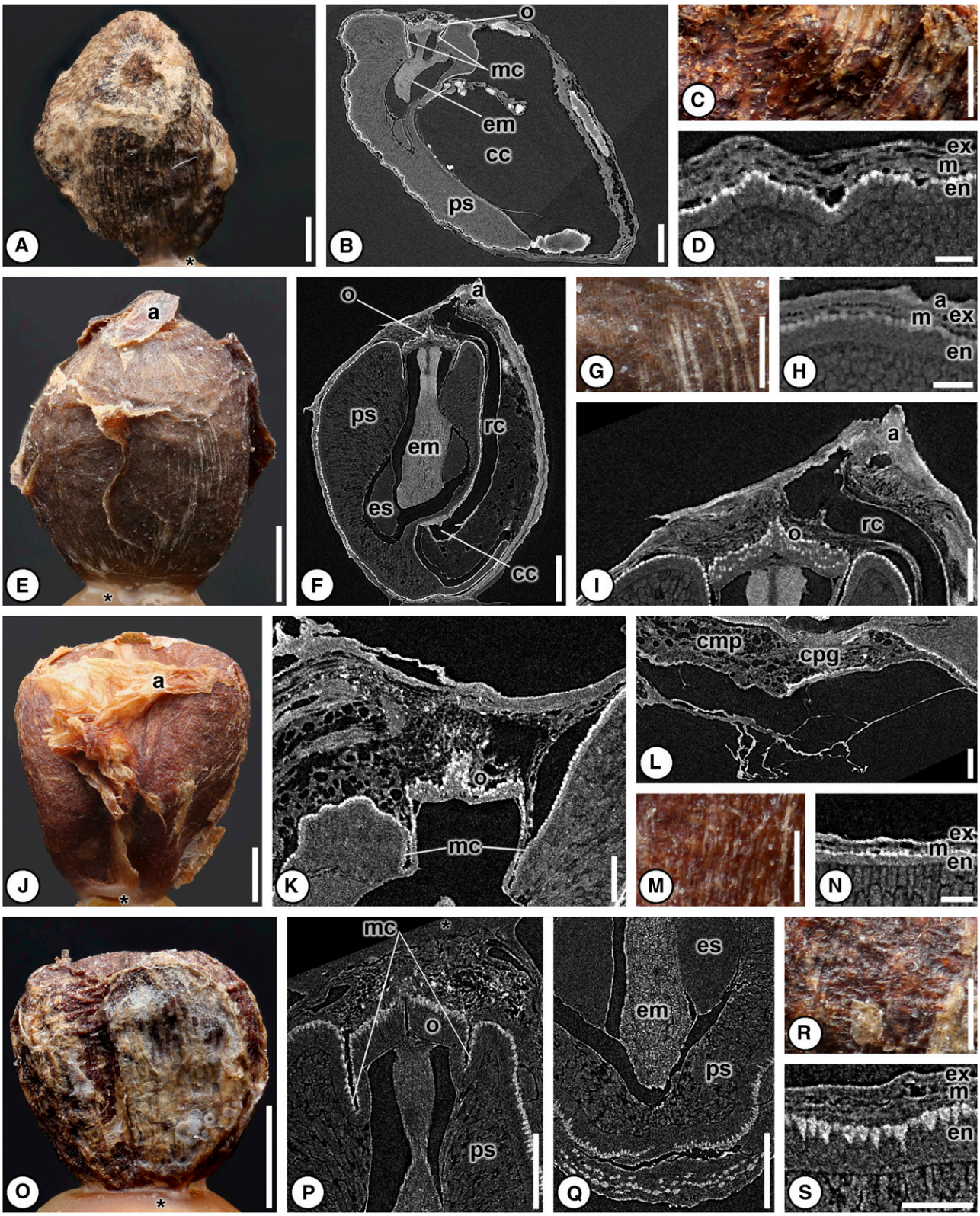

FIGURE 6 Seed anatomy in subfamily Alpinioideae, tribe Alpinieae. A, C, E, G, J, M, O, R: light micrographs; B, F, I, K–L, P–Q: digital longitudinal sections; D, H, N, S: digital transverse sections. (A–D) *Alpinia rafflesiana*. (A) Overview of dark brown seed with aril enveloping seed and tightly adpressed to seed coat. (B) Seed with *Amomum*-like chalazal chamber (cc), perisperm (ps), embryo with forked base (em), and multilayered operculum (o) at micropylar region of seed nested within micropylar collar (mc). (C) Detail of verrucose seed surface. (D) Testa with poorly developed exotesta (ex), single type of mesotestal cells (m), and endotesta of elongate sclerenchyma (en). (E–I) *Elettariopsis unifolia*. (E) Overview of dark brown seed surface with aril (a) fully

both perisperm and endosperm and variation in embryo shape and testa) enables recognition of multiple characters and character states not available in plant groups with simpler seed organization. In addition, the use of nondestructive SRXTM substantially increases confidence in the assessment of characters because artifacts of physical sectioning (such as tears within tissues caused by sectioning, spaces linked to shrinkage during embedding, and distortion linked to different tissue response to sectioning or embedding media) are all avoided (a point emphasized by Smith et al., 2009). The only artifacts that need to be taken into account are those of shrinkage and distortion during seed drying naturally or for herbarium preparation, which were accounted for because all scanned seeds were dry before scanning. Furthermore, the ability to examine multiple planes of section in SRXTM data sets reinforces character state documentation. Thus, in combination, seed complexity and observation by SRXTM provide a powerful tool for phylogenetic analyses by yielding multiple characters and character states that can be applied in evaluating relationships within Zingiberaceae.

While no single seed character state was found to be unique to any single subfamily, combinations of seed character states were found that can be used to distinguish between the three subfamilies Alpinioideae [absence of a multiseriate exotesta (29), short to elongate sclerified endotesta (31), and a nondiscoid chalazal pigment group (33)], Siphonochiloideae [a solid aril (4), an externally visible raphe (10), and lack of a micropylar collar (15)], and Zingiberoideae [lack of an externally visible raphe (10), a hilar rim of exotesta and mesotesta (19 and 20), no columnar chalazal proliferations (23), no chalazal mucro (25), seed coat 100–199 μm in thickness (26), an endotesta of thin parenchyma (31), an endotestal gap at the base of the seed (32), a discoid chalazal pigment group (33), and embryos that do not contact the testa (38)] (Table 3; Fig. 10A–B). In contrast, at the tribal level, the only tribe with a unique combination of character states not possessed by any other taxon outside of the tribe was Globbeae; Alpinieae, Riedelieae, and Zingibereae were found to have distinctive characters to support the tribes, but these characters or character states were also occasionally found in taxa outside the tribe.

Of the 39 characters analyzed, 22 were found to be informative for distinguishing the subfamilies and tribes as currently recognized, whereas 17 were found to be variable at both the subfamily and tribal level and are not useful for distinguishing tribes or subfamilies (Table 3). The informative characters that allowed for differentiation of the tribes and subfamilies are seed color (1), trichomes on seed coat or aril (3), aril type (4), an externally visible raphe (10), an external chalazal indentation (11), an operculum (13), a micropylar collar (15), a hilar rim (19), the layering of the hilar rim (20), a columnar chalazal testal proliferation (23), a chalazal chamber (24), a chalazal mucro (25), the thickness of the testa (26), a uniform exotesta (28), a multiseriate exotesta (29), the shape of the endotestal cells (31), the location of an endotestal gap (32), a chalazal pigment group (33), the length of the embryo (35), differentiation of the embryo base (37), contact of the embryo with the endotesta (38), and basally proliferated endosperm (39). Uninformative characters that were either too variable within a group or commonly found among different groups are: the surface of the seed (2), the shape of the seed (5), seed contortion (6), seed length (7), tapering of the seed body at the micropyle (8), tapering of the seed at the chalaza (9), the shape of the micropylar region (12), the layering of the operculum (14), the layering of the micropylar collar (16), a thickened micropylar collar (17), a recurved micropylar collar (18), a micropylar mesotesta proliferation of cells (21), massive chalazal testal proliferations (22), the type of exotestal cells (27), the number of types of mesotestal cells (30), the raphe canal (34), and the shape of the embryo (36).

Siphonochiloideae—The two genera of Siphonochiloideae shared a mosaic of character states with members of Alpinioideae and Zingiberoideae, which is not surprising as they are sister to the rest of the Zingiberaceae (Kress et al., 2002; Fig. 10B). Some members of both Siphonochiloideae and Alpinioideae have a distinctive externally visible raphe (10) and embryos that touch the endotesta (38), two characters lacking in all Zingiberoideae. All members of Siphonochiloideae analyzed and some Zingiberoideae have a parenchymatous endotesta (31), a discoid-shaped chalazal pigment group (33), and are lacking any evidence of a micropylar collar (15), which is in direct contrast to Alpinioideae, where not a single member lacks a micropylar collar (15) and all members have a sclerenchymatous endotesta (31) and trumped-shaped chalazal pigment group (33).

Zingiberoideae—Zingiberoideae seeds show a unique combination of 10 character states (Table 3). Two of these character states, an endotesta of parenchymatous cells (31) and a discoid-shaped chalazal pigment group (33) have been previously used to unite the

←

enveloping seed and tightly adpressed to seed coat. (F) Seed showing aril (a), elongated J-shaped embryo with bulbous base (em), perisperm (ps), abundant, basally proliferated endosperm (es), and distinctive raphe canal (rc) terminating in *Amomum*-type chalazal chamber (cc). (G) Detail of dark brown striate seed coat covered by thin translucent aril. (H) Testa with amorphous arillate tissue (a), cuboidal exotesta (ex), one type of mesotestal cells (m), and thick layer of large palisade endotestal cells (en). (I) Micropylar region with multilayered operculum (o), arillate tissue (a), and large raphe canal (rc) originating at micropyle. (J–N) *Geocharis aurantiaca*. (J) Overview of red to light brown seed coat and aril (a) enveloping entire seed and tightly adpressed to seed coat. (K) Micropylar region with multilayered operculum (o) and micropylar collar (mc) formed from endotesta only. (L) Chalazal region with nondiscoid-shaped chalazal pigment group (cpg) and chalazal mesotestal proliferations (cmp). (M) Detail of seed coat showing striations obscured slightly by translucent aril. (N) Testa with poorly developed exotesta (ex), two types of mesotestal cells (m), and endotesta of elongate sclerenchyma (en). (O–S) *Hornstedtia scottiana*. (O) Overview of dark brown seed enveloped by translucent aril tightly adpressed to seed coat. (P) Micropylar region with multilayered operculum (o) and micropylar collar of endotestal cells only (mc) nested within perisperm (ps). (Q) Chalazal region with elongated embryo (em), perisperm (ps), and abundant, basally proliferated endosperm (es). (R) Detail of verrucose and striate seed surface slightly obscured by translucent aril. (S) Testa with poorly developed exotesta (ex), two types of mesotestal cells (m), and endotesta of elongate sclerenchyma cells (en). Scale bars: A, E, J, O = 1 mm; B, F = 500 μm; C, G, I, K–M, P–R = 250 μm; D, H, N, S = 100 μm. * mounting glue and specimen stub.

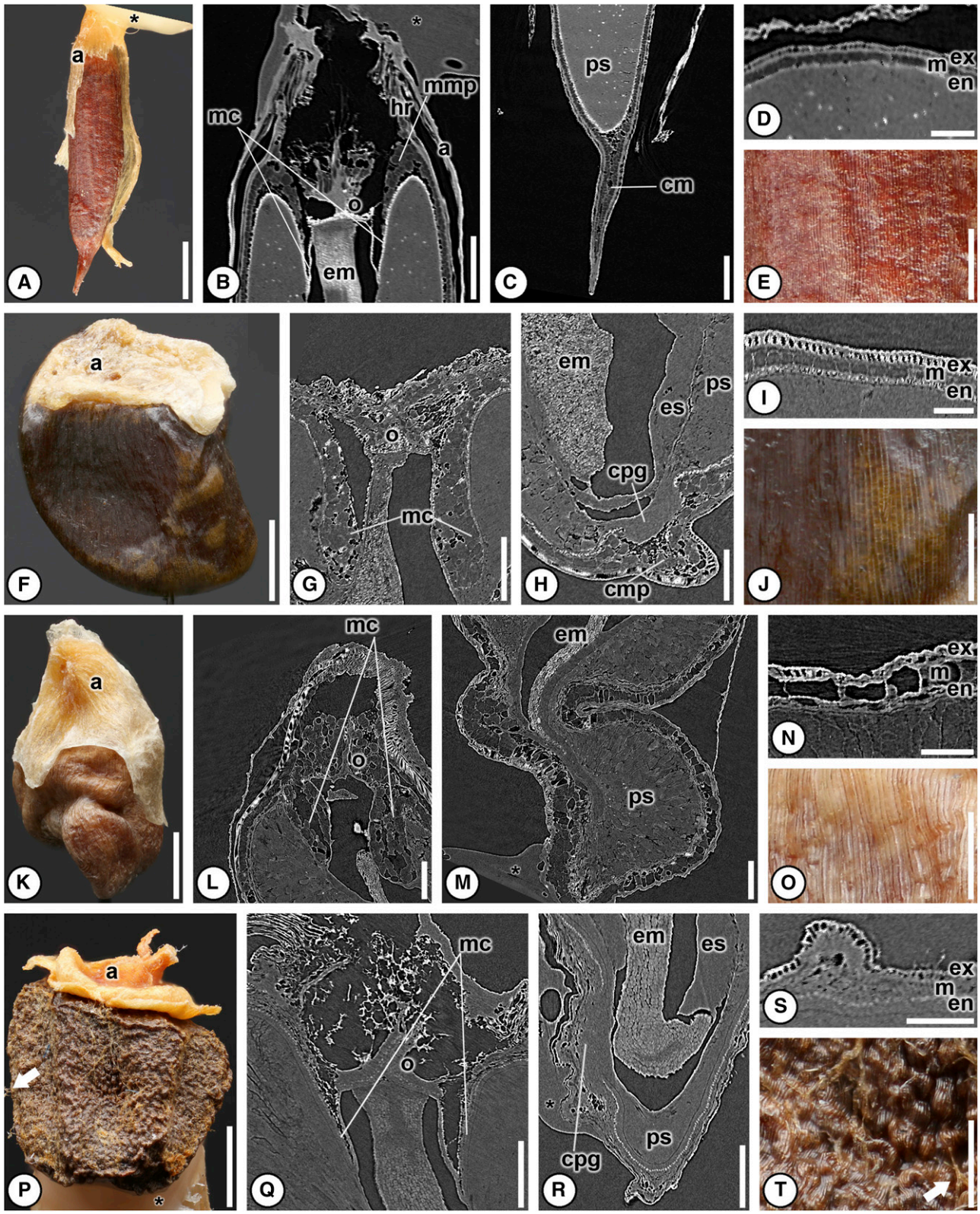

FIGURE 7 Seed anatomy in subfamily Alpinioideae, tribe Riedelieae. A, E–F, J–K, O–P, T: light micrographs; B–C, G–H, L–M, Q–R: digital longitudinal sections; D, I, N, S: digital transverse sections. (A–E) *Burbidgea stenantha*. (A) Overview of red seed with aril (a) divided into thin strands and chalazal mucro. Note: some strands of aril were removed to show seed body. (B) Micropylar region showing aril (a), hilar rim formed from exotesta (hr), bulbous micropylar mesotestal proliferations (mmp), multilayered operculum (o), micropylar collar (mc) of endotestal cells only, and embryo (em). (C) Chalazal region showing abundant perisperm (ps) and chalazal mucro (cm) at base of seed. (D) Testa with palisade exotestal cells (ex), two types of mesotestal

subfamily (Liao and Wu, 2000) and are reported here for the first time in the previously unstudied genera *Boesenbergia*, *Camptandra*, *Distichochlamys*, *Newmania*, *Gagnepainia*, and *Hemiorchis* (Liao and Wu, 2000). Interestingly, the two aforementioned character states are also found within the earliest-diverging lineage of Zingiberaceae, Siphonochiloideae. The other 10 character states, introduced here for the first time, help reinforce the relationships of members of the Zingiberoideae.

The Globbeae were found to possess a unique combination of 16 character states in the seven species analyzed, and a combination of three character states—a light-colored seed (1), the presence of trichomes (3), and an undifferentiated embryo base (37)—can be used to distinguish the tribe from other Zingiberaceae. *Boesenbergia curtisii* (Baker) Schltr. was very similar to Globbeae members, but differed in having a white seed (36), where all Globbeae seeds are either red or tan and never white or black. *Newmania* and *Monolophus sikkimensis* were also similar to Globbeae, but differed in having a bulbously differentiated embryo base, a character not seen in Globbeae. It was reported previously that Zingibereae (then separated into Hedychieae and Zingibereae) can be distinguished from Globbeae on the basis that *Globba racemosa* Sm. has a multiseriate exotesta (Liao and Wu, 2000), but in our expanded sampling of the tribe including all three genera, it was found that a multiseriate exotesta (29) is lacking in *Globba spathulata*, *Gagnepainia harmandii*, and *Hemiorchis* sp., thus eliminating the utility of this character to separate the Globbeae from the Zingibereae.

The Zingibereae share 13 character states in common for the 18 species analyzed (Table 3), but these character states are not unique to Zingibereae, as *Globba spathulata* has an identical combination of character states for the same 13 characters. The other members of Globbeae differ from Zingibereae in either possessing an external chalazal indentation (*Hemiorchis* and *Gagnepainia harmandii*) or a multiseriate exotesta (*Globba pendula*, *G. sessiliflora* Sims, *G. aurea* Elmer, and *G. maculata* Blume).

Alpinioideae—Seed morphoanatomy is extraordinarily diverse (see Benedict et al., 2015 for discussion), but a combination of two character states unites the subfamily: a uniseriate exotesta (29) and a nondiscoid chalazal pigment group (33). A nondiscoid chalazal pigment group (33) and sclerenchymatous endotesta (31) were originally reported by Liao and Wu (2000) in five genera (*Alpinia*, *Amomum*, *Etlingera*, *Hornstedtia*, and *Plagiostachys*) and 43 species to unite the subfamily and corroborated by Benedict et al. (2015) in a broader analysis of the subfamily that included *Aframomum* spp., *Burbidgea stenantha*, *Geocharis aurantiaca* Ridl., *Geostachys densiflora* Ridl., *Pleuranthodium* sp., *Renealmia* spp., *Siamanthus siliquosus*, *Siliquamomum tonkinense*, and *Vanoverberghia sepulchrei* Merr. We have since sampled more Alpinioideae (introduced here) including more species of *Alpinia*, *Aframomum*, and *Hornstedtia*, and *Elettariopsis unifolia* (Gagnep.) M.F.Newman and have found the characters mentioned above to be consistent in all Alpinioideae examined. It is important to note that our endotesta character (31) includes thickness, cell shape, and cell type and is not directly equivalent to the character of Liao and Wu (2000). It is consistent with respect to a sclerenchymatous or parenchymatous cell type; however, cells vary in thickness within the subfamily.

The Alpinieae share seven character states among the 40 species analyzed (Table 3), but the combination of these character states is not unique to the tribe. *Pleuranthodium* (Riedelieae) is identical with respect to these character states, while *Siamanthus siliquosus* (Riedelieae) is similar to Alpinieae taxa but is easily distinguished by conspicuous trichomes (3) on the exotesta, a character lacking in all Alpinieae. *Riedelia* spp. and *Burbidgea stenantha* (Riedelieae) are also similar in morphoanatomy with Alpinieae, but lack a well-formed basally proliferated endosperm (39).

Five species representing the four genera of Riedelieae were analyzed and are found to share 12 character states. However, the combination of these characters is not unique to Riedelieae and is also found in *Vanoverberghia sepulchrei* (Alpinieae). It is notable that all studied members of Riedelieae lack a chalazal chamber (24), which is often present in seeds of Alpinieae.

***Unplaced taxa:* Siliquamomum tonkinense *and* Monolophus sikkimensis**—In recent studies based on molecular data, *Siliquamomum tonkinense* was placed as either sister to the *Alpinia rafflesiana* clade, which was then sister to the remaining Alpinieae (Kress et al., 2005) or in a polytomy with Riedelieae and the rest of Alpinieae (sensu Kress et al., 2007), or with low bootstrap support (<50%) as the earliest-diverging lineage sister to the rest of Riedelieae (sensu Kress et al., 2002). When seed morphoanatomical character states of *Siliquamomum tonkinense* were analyzed, one character state, an externally visible raphe (10), was found in some members of Alpinieae, but not in any Riedelieae, and three character states [the presence of trichomes (3), a chalazal mucro (25), and weak basally proliferated endosperm (39)] were found to ally it with members of

cells, one bulbous, the other very thin (m), and endotesta of short sclerenchyma (en). (E) Detail of striate seed surface. (F–J) *Pleuranthodium* sp. (F) Overview of dark brown seed with arillate tissue (a) at micropylar region of seed. (G) Micropylar region showing a multilayered operculum (o) nested within thickened micropylar collar (mc) formed from both endotestal and mesotestal cells. (H) Chalazal region with elongated embryo (em), abundant, basally proliferated endosperm (es), perisperm (ps), chalazal mesotestal proliferation of cells (cmp), and nondiscoid chalazal pigment group (cpg). (I) Transverse section of testa with palisade exotesta (ex), two types of mesotestal cells (m), and endotesta of short sclerenchyma cells (en). (J) Detail of striate seed coat. (K–O) *Riedelia corallina*. (K) Overview of tan seed partially enveloped by light yellow aril (a). (L) Micropylar region showing a multilayered operculum (o) resting on top of thickened micropylar collar (mc) formed from mesotestal and endotestal cells. (M) Chalazal region with J-shaped, elongated embryo (em) and abundant perisperm (ps). (N) Testa showing palisade exotesta (ex), two types of mesotestal cells (m), and endotesta of short sclerenchyma (en). (O) Detail of striate seed surface. (P–T) *Siamanthus siliquosus*. (P) Overview of dark brown seed with solid yellow aril (a) and trichomes (arrow). (Q) Micropylar region with multilayered operculum (o) and micropylar collar (mc) formed from endotesta. (R) Chalazal region showing J-shaped embryo (em), abundant, basally proliferated endosperm (es), perisperm (ps), and nondiscoid-shaped chalazal pigment group (cpg). (S) Testa with palisade exotesta (ex), two types of mesotestal cells (m), and endotesta of short sclerenchyma (en). (T) Detail of verrucose seed surface with trichomes (arrow). Scale bars: A, F, K, P = 1 mm; B–C, E, G–H, J, L–M, O, Q–R, T = 250 μm; D, I, N, S = 100 μm. * mounting glue and specimen stub.

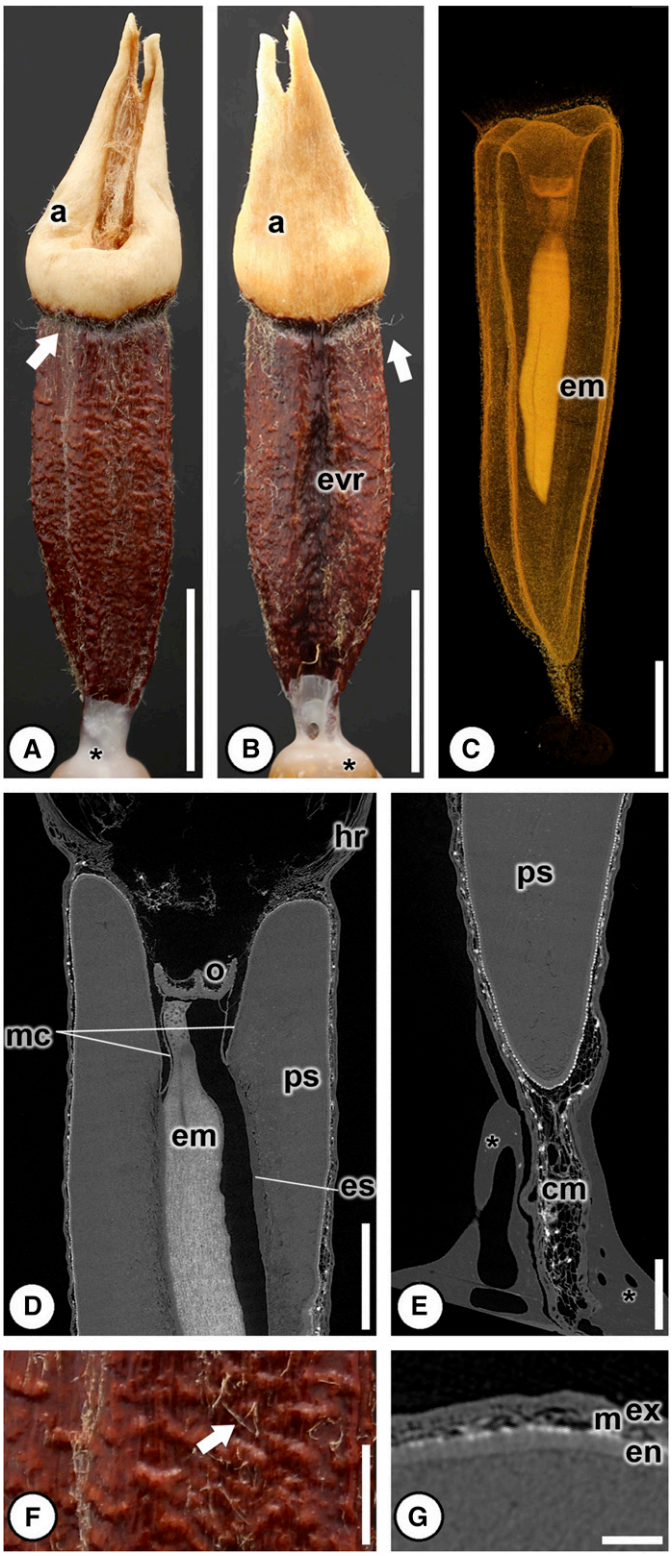

FIGURE 8 Seed anatomy of *Siliquamomum tonkinense* (Alpinioideae). A–B, F: light micrographs; C: 3D volume rendering; D–E: digital longitudinal sections; G: digital transverse section. (A) Overview of elongate, red seed with trichomes (arrow), and tan aril divided into two thick lobes (a). (B) Overview of elongate, red seed with trichomes (arrow), tan aril (a), and externally visible raphe (evr). (C) 3D volume rendering showing internal part of seed with elongated, straight embryo (em). (D) Micropylar region with hilar rim formed from endotestal and mesotestal cells (hr), single-layered operculum (o), micropylar collar (mc) formed from both endotestal and mesotestal cells, embryo (em), perisperm (ps), and abundant, basally proliferated endosperm (es). (E) Chalazal region with perisperm (ps) and chalazal mucro (cm) of exotesta and mesotesta. (F) Detail of verrucose seed surface covered in trichomes (arrow). (G) Testa with palisade exotesta (ex), two types of mesotestal cells (m), and elongate sclerenchyma (en). Scale bars: A–B = 5 mm; C = 2 mm; D = 250 µm; E–F = 1 mm; G = 100 µm. * mounting glue and specimen stub.

Riedelieae. Additionally, when *Siliquamomum tonkinense* was compared with Alpinioideae taxa surveyed here, it was found to be most similar to *Burbidgea stenantha*, sharing 31 of the 39 seed character states analyzed. In parsimony analyses, both with and without added characters from DNA sequence data, *Siliquamomum tonkinense* is shown to be closely related to *Burbidgea* and never sister to *Alpinia rafflesiana*, as suggested by previous authors (data not shown). In fact, only 17 of the 39 seed characters are shared between the latter two taxa, the lowest number of characters shared between any Alpinioideae and *Siliquamomum tonkinense* (Table 3). On the basis of the available morphological and molecular data, it is most parsimonious to conclude that *Siliquamomum* be included as a member of Riedelieae, but more morphological and molecular data are needed confirm its relationship with either tribe.

Monolophus is the only genus currently unplaced in the Zingiberoideae based on a combined ITS and *matK* data set (Kress et al., 2002). Larsen and Smith (1972) postulated a close relationship with *Camptandra* and *Boesenbergia*, but that was not supported based on molecular work, and the genus remains unplaced (Kress et al., 2002). Seeds of *Monolophus sikkimensis* were analyzed and compared with other Zingiberoideae and found to have one character state unique to Globbeae, a single type of mesotestal cells (30), and two character states indicative of Zingibereae, a poorly developed exotesta (27) and a bulbous embryo (37). Although further information is needed to make a formal placement of *Monolophus*, it may be more closely related to Zingibereae based on our reported seed characters.

Notable character state changes in Zingiberaceae—Certain characteristics of Zingiberaceae seeds have many character state reversals within the family, creating a large number of homoplasious characters and character states; however, other characters show less homoplasy and are useful in separating formally recognized clades (Table 3). The most useful characters for supporting currently recognized formal and informal clades are those relating to the endotestal cells (31) and the type of chalazal pigment group (33), also derived from the endotesta (Fig. 11). The endotesta has a single shift from thin and parenchymatous in Siphonochiloideae and Zingiberoideae to sclerified of various thicknesses in Alpinioideae with no reversals to parenchymatous cells (Fig. 11). The chalazal pigment group (33) is discoid in Siphonochiloideae and Zingiberoideae, but is nondiscoid in Alpinioideae, suggesting a single shift in Alpinioideae (Fig. 11). Trichomes on the seed coat or aril (3) have perhaps been gained twice in Alpinioideae (*Siamanthus siliquosus* and *Siliquamomum tonkinense*), and have been lost in at least three lineages in the Zingiberoideae (Fig. 12). Larsen (2002)

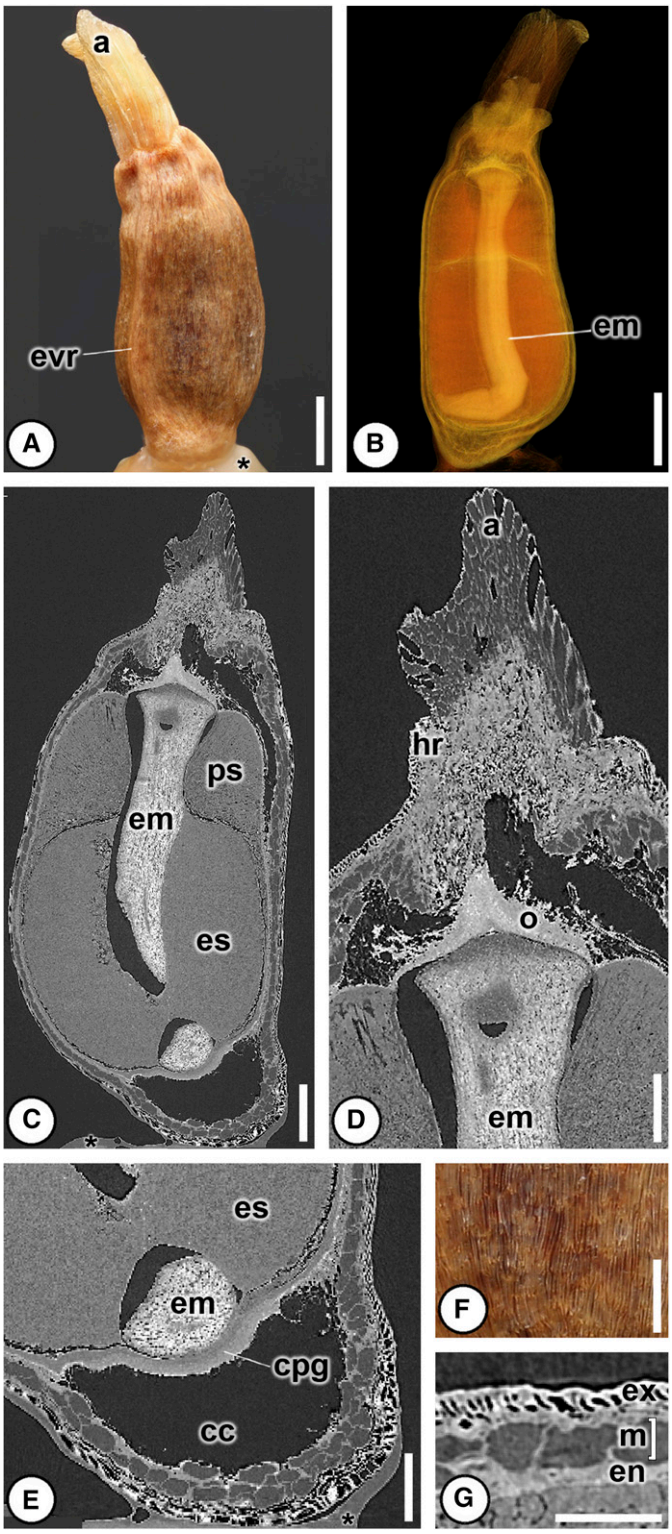

FIGURE 9 Seed anatomy of *Siphonochilus aethiopicus* (Siphonochiloideae). A, F: light micrographs; B: 3D volume rendering; C–E: digital longitudinal sections; G: digital transverse section. (A) Overview of light brown seed with aril (a) and externally visible raphe (erg). (B) 3D volume rendering showing internal shape of seed with elongated, J-shaped embryo (em). (C) Overview of entire seed with embryo (em) nested within perisperm (ps) and abundant, basally proliferated endosperm (es). (D) Micropylar region of seed with hilar rim (hr) of exotesta and mesotesta situated below aril tissue (a) and above single-layered operculum (o) and embryo (em). (E) Chalazal region with *Alpinia*-type chalazal chamber (cc), discoid-shaped chalazal pigment group (cpg), abundant, basally proliferated endosperm (es) and embryo (em) touching endotesta. (F) Detail of striate surface of the seed coat. (G) Detail of testa with nonuniform palisade exotesta (ex), two types of mesotestal cells (m), and endotesta of square to parenchyma cells (en). Scale bars: A, B = 1 mm; C = 500 µm; D–F = 250 µm; G = 100 µm. * mounting glue and specimen stub.

suggested that the trichomes found on some *Monolophus* create air pockets so they can be abiotically dispersed by water, which would be an interesting ecological explanation for the multiple originations of trichomes in Zingiberaceae seeds. The micropylar collar (15) was previously shown by Liao and Wu (2000) to be lost in *Cautleya gracilis* and *Monolophus coenobialis* Hance [as *Caulokaempferia coenobialis* (Hance) K.Larsen], which we confirm, and we have documented additional instances of loss of micropylar collar (Fig. 12). It was lost at least once in Globbeae (*Globba spathulata*), again in Zingibereae (*Camptandra ovata*), and in Siphonochiloideae (Fig. 12). Interestingly all these seeds, except those of members of Siphonochiloideae, are very small (1–2 mm), so the loss of the micropylar collar could be attributed to reduction in seed size, but its absence in the large seeds of *Siphonochilus aethiopicus* (>5 mm) refutes this idea. Loss of micropylar collar also does not correlate with the loss of an operculum, because all taxa studied here without a micropylar collar still possess an operculum. Further investigations into the functional roles of trichomes and the micropylar collar are needed.

CONCLUSIONS

Zingiberaceae seeds are morphologically and anatomically diverse and possess a large number of systematically significant characters. Many of the characters used here are novel and have the potential to be applied to other seed-bearing plants with similar structural complexity. The use of nondestructive SRXTM substantially increases confidence in the assessment of characters because complications and artifacts arising from physical sectioning are avoided. SRXTM also provides the ability to investigate rare and/or endangered taxa from herbaria, which is useful for future studies centered on seed or fruit morphoanatomy because these are sometimes less common in collections as compared with flowering specimens. Thirty-nine characters were analyzed for 75 species within Zingiberaceae, and 22 characters were found to be useful for differentiating the subfamilies and tribes as currently described. Using a combination of characters, we could distinguish the subfamilies Alpinioideae, Zingiberoideae, and Siphonochiloideae using seed morphoanatomy. Globbeae were the only tribe found to possess a unique combination of character states not seen in any species outside the tribe. The lack of seed character states that unite the other tribes may be due to a significant amount of homoplasy, but seed features are still useful in combination with other morphological characters to determine synapomorphies for the various clades, documenting the importance of widely surveying plant groups for novel characters not previously used in classification studies. The seed character states of currently unplaced genera

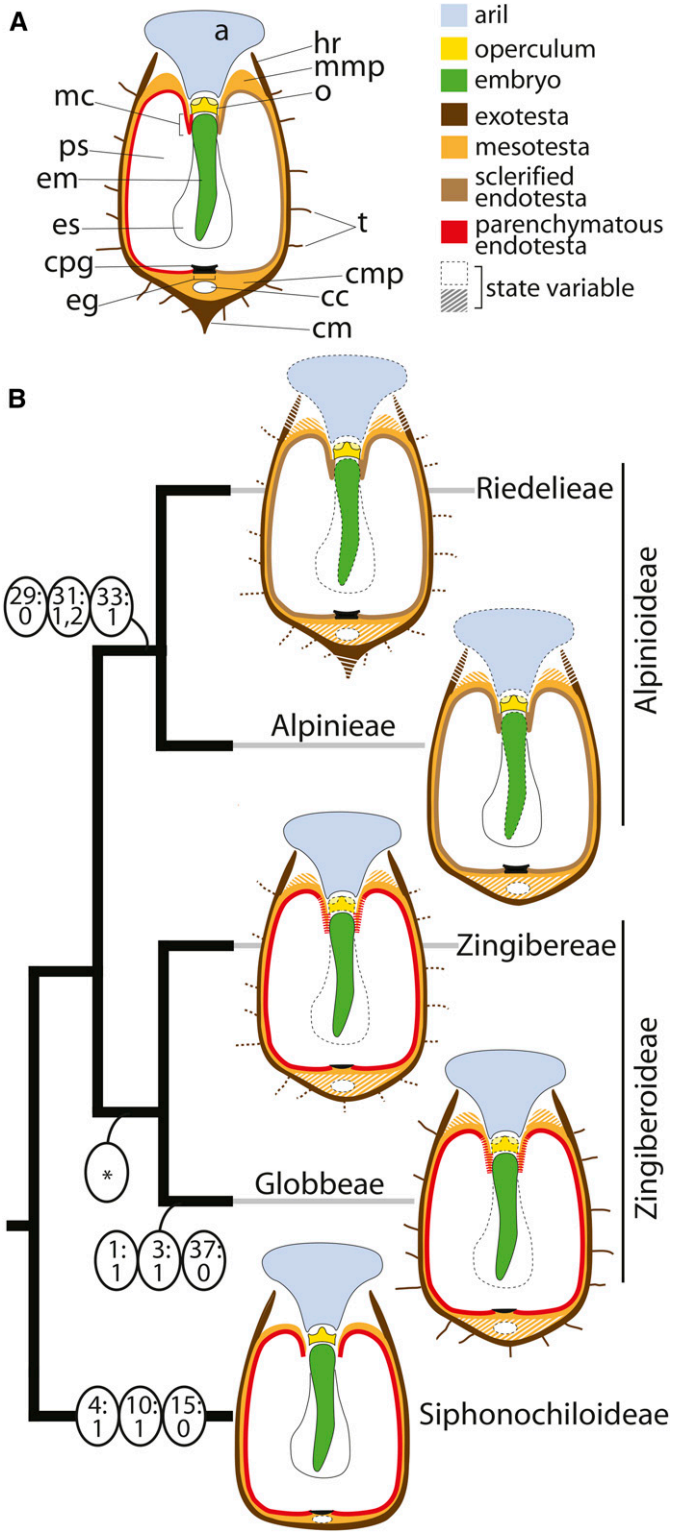

FIGURE 10 Generalized diagrams of seeds on a cladogram of Zingiberaceae based on Wood et al. (2000), Kress et al. (2002, 2007) and Leong-Škorničková et al. (2011). *Abbreviations:* aril (a), hilar rim (hr), micropylar mesotestal proliferation of cells (mmp), operculum (o), trichomes (t), chalazal mesotestal proliferation of cells (cmp), chalazal chamber (cc), chalazal mucro (cm), endotestal gap (eg), chalazal pigment group (cpg), endosperm (es), embryo (em), perisperm (ps), micropylar collar (mc). Characters uniting various clades are as follows (character: character state): Alpinioideae, no multicellular exotesta (29: 0), short or elongate sclerified endotesta (31: 1, 2), nondiscoid chalazal pigment group (33: 1); Zingiberoideae (at asterisk) lack of an externally visible raphe (10: 0), a hilar rim of exotesta and mesotesta (19: 1 and 20: 1), no columnar chalazal proliferations (23: 0), no chalazal mucro (25: 0), seed coat 100–199 µm in thickness (26: 1), an endotesta of thin parenchyma (31: 0), an endotestal gap at the base of the seed (32: 0), a discoid chalazal pigment group (33: 0), and embryos that do not contact the testa (38: 0); Globbeae, light-colored seeds (1: 1), trichomes on aril or seed coat (3: 1), an undifferentiated embryo base (37: 0); Siphonochiloideae, a solid aril (4: 1), an externally visible raphe (10: 1), and lack of a micropylar collar (15: 0).

within Zingiberaceae, *Monolophus* and *Siliquamomum*, have been compared with those of other taxa within the family and suggest that *Siliquamomum* may be related to Riedelieae, and *Monolophus* to Zingibereae. However, more data are needed to formally revise the family. The Zingiberaceae are a large family with considerable morphological and anatomical variation in both reproductive and vegetative characters. The research presented here demonstrates the utility of using seed characters to independently test hypotheses of evolutionary relationships. Further, morphological studies like this are critical to understanding long-term evolutionary patterns where the fossil record will be considered because no DNA data are available for these extinct taxa.

ACKNOWLEDGEMENTS

The authors thank A. Reznicek (MICH), W. J. Kress, I. Lopez, and J. Wen (US), W. Friedrich (Aarhus University), and J. Kallunki and S. Sylva (NY) for facilitating access to material that formed part of this study, and M. Andrew, G. Benson-Martin, S. Brown, J. Defontes, J. Dorey, J. L. Fife, S. Joomun, S. Little, A. Pineyro, S. McKechnie, K. Morioka, M. Ng, B. Robson, N. Sheldon, and R. Yockteng for help at the beamlines. This work was supported by a Heliconia Society International award to J.C.B. and National Science Foundation grants DEB 1257080 (S.Y.S) and 1257701 (C.D.S). Research of J.L.S. is supported by National Parks Board, Singapore and the Czech Science Foundation, GAČR P506-14-13541S. A portion of this work was included in the dissertation of J.C.B. mentored by K. B. Pigg, whom J.C.B. thanks. The research at the TOMCAT beamline at the Swiss Light Source, Paul Scherrer Institut, Villigen, Switzerland received funding from Integrated Infrastructure Initiative (I3) on Synchrotrons and FELs and the European Community's Seventh Framework Program (FP7/2007–2013) under grant agreement n.°312284 (CALIPSO) through SLS to M.E.C. and S.Y.S. This research used resources of the Advanced Photon Source, a U.S. Department of Energy (DOE) Office of Science User Facility operated for the DOE Office of Science by Argonne National Laboratory under Contract No. DE-AC02-06CH11357. The Advanced Light Source is supported by the Director, Office of Science, Office of Basic Energy Sciences, of the U.S. Department of Energy under Contract No. DE-AC02-05CH11231. The authors thank the editor, Linda M. (Prince) MacKechnie, and an anonymous reviewer for constructive and helpful comments.

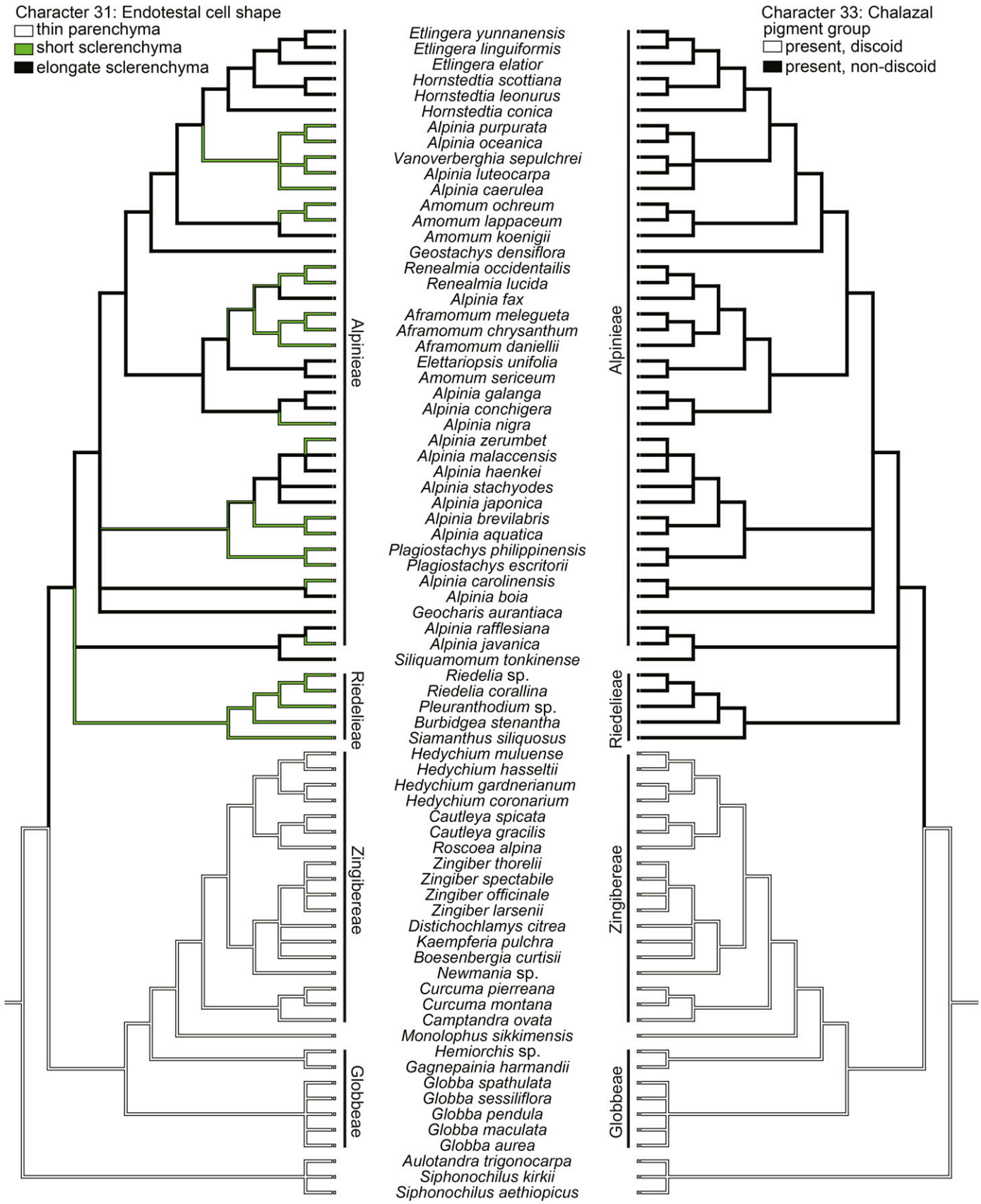

FIGURE 11 Two cladograms showing the distribution and ancestral state reconstruction of endotestal cell type and shape (character 31) and chalazal pigment group (character 33) characters within Zingiberaceae.

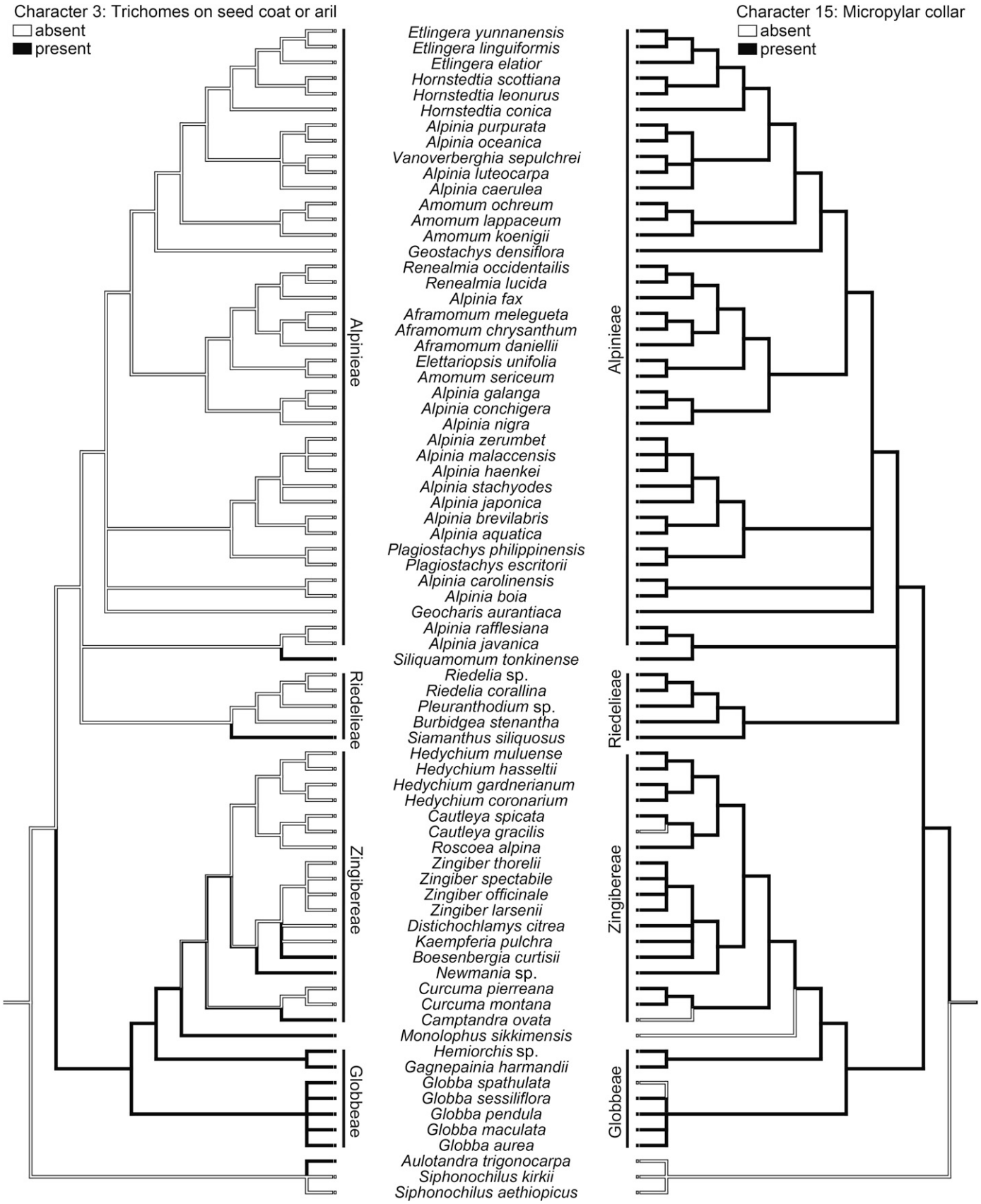

FIGURE 12 Two cladograms showing the distribution and ancestral state reconstruction of trichomes on seed coat or aril (character 3) and micropylar collar (character 15) within Zingiberaceae.

LITERATURE CITED

Baskin, C. C., and J. M. Baskin. 2001. Seeds, ecology, biogeography, and evolution of dormancy and germination. Elsevier, San Diego, California, USA.

Benedict, J. C. 2012. Zingiberalean fossils from the Late Paleocene of North Dakota, USA and their significance to the origin and diversification of Zingiberales. Ph.D. dissertation, Arizona State University, Tempe, Arizona, USA.

Benedict, J. C., S. Y. Smith, M. E. Collinson, J. Leong-Škorničková, C. D. Specht, J. L. Fife, F. Marone, X. Xiao, and D. Y. Parkinson. 2015. Evolutionary significance of seed structure in Alpinioideae (Zingiberaceae). *Botanical Journal of the Linnean Society*.

Boesewinkel, F. D., and F. Bouman. 1995. The seed: Structure and function. *In* J. Kigel and G. Galili [eds.], Seed development and germination, 1–24. Marcel Dekker, New York, New York, USA.

Burtt, B. L., and R. M. Smith. 1972. Key species in the taxonomic history of Zingiberaceae. *Notes from the Royal Botanical Garden Edinburgh* (31)2: 177–227.

Chen, I., and S. R. Manchester. 2007. Seed morphology of modern and fossil *Ampelocissus* (Vitaceae) and implications for phytogeography. 2007. *American Journal of Botany* 94: 1534–1553.

Collinson, M. E., S. R. Manchester, and V. Wilde. 2012. Fossil fruits and seeds of the Middle Eocene Messel biota, Germany. *Abhandlungen der Senckenberg Gesellschaft für Naturforschung* 570: 1–249.

Collinson, M. E., and P. F. van Bergen. 2004. Evolution of angiosperm fruit and seed dispersal biology and ecophysiology: Morphological, anatomical and chemical evidence from fossils. *In* A. R. Hemsley and I. Poole [eds.], The evolution of plant physiology, Linnean Society Symposium Series no. 21, 323–377. Elsevier, London, UK.

Corner, E. J. H. 1976. The seeds of dicotyledons, vols. 1 and 2. Cambridge University Press, Cambridge, UK.

Dowd, B. A., G. H. Campbell, R. B. Marr, V. Nagarkar, S. Tipnis, L. Axe, and D. P. Siddons. 1999. Developments in synchrotron x-ray computed microtomography at the National Synchrotron Light Source. *Proceedings of the Society for Photo-Instrumentation Engineers* 3772: 224–236.

Grootjen, C. J., and F. Bouman. 1981. Development of the ovule and seed in *Costus cuspidatus*, with special reference to the formation of the operculum. *Botanical Journal of the Linnean Society* 83: 27–39.

Harris, D. J., A. D. Poulsen, C. Frimodt-Møller, J. Preston, and Q. C. B. Cronk. 2000. Rapid radiation in *Aframomum* (Zingiberaceae): Evidence from nuclear ribosomal DNA internal transcribed spacer (ITS) sequences. *Edinburgh Journal of Botany* 57: 377–395.

Herrera, F., S. R. Manchester, M. R. Carvalho, C. Jaramillo, and S. L. Wing. 2014. Paleocene wind-dispersed fruits and seeds from Colombia and their implications for early Neotropical rainforests. *Acta Palaeobotanica* 54: 197–229.

Holttum, R. E. 1950. The Zingiberaceae of the Malay Peninsula. *Gardener's Bulletin Singapore* 13: 1–249.

Humphrey, J. E. 1896. The development of the seed in the Scitamineae. *Annals of Botany* 37: 1–40.

IPNI. 2015. International plant names index. Website http://www.ipni.org [accessed 22 May 2015].

Kapil, R. N., J. Bor, and F. Bouman. 1980. Seed appendages in angiosperms. I. Introduction. *Botanische Jahrbucher fur Systematik, Pflanzengeschichte und Pflanzengeographie* 101: 555–573.

Kimura, Y., and M. Yoshimura. 1968. On the identification of cardamoms found in drug markets of Eastern Asia. *Journal of Japanese Botany* 44(3): 65–70.

Kress, W.J. 1990. The phylogeny and classification of the Zingiberales. *Annals of the Missouri Botanical Garden* 77: 698–721.

Kress, W. J. 1996. Phylogeny of the Zingiberanae: Morphology and molecules. *In* T. L. Wu, Q. G. Wu, and Z. Y. Chen [eds.], Proceedings of the 2nd Symposium on the Family Zingiberaceae, 122–141. Zhongshan University Press, Guangzhou, China.

Kress, W. J., A.-Z. Liu, M. Newman, and Q.-J. Li. 2005. The molecular phylogeny of *Alpinia* (Zingiberaceae): a complex and polyphyletic genus of gingers. *American Journal of Botany* 92: 167–178.

Kress, W. J., M. F. Newman, A. D. Poulsen, and C. D. Specht. 2007. An analysis of generic circumscriptions in tribe Alpinieae (Alpinioideae: Zingiberaceae). *Gardens' Bulletin Singapore* 59: 113–128.

Kress, W. J., L. M. Prince, W. J. Hahn, and E. A. Zimmer. 2001. Unraveling the evolutionary radiation of the families of Zingiberales using morphological and molecular evidence. *Systematic Biology* 50: 926–944.

Kress, W. J., L. M. Prince, and K. J. Williams. 2002. The phylogeny and a new classification of the gingers (Zingiberaceae): Evidence from molecular data. *American Journal of Botany* 89: 1682–1696.

Larsen, K. 2002. Three new species of *Caulokaempferia* (Zingiberaceae) from Thailand with a discussion of the generic diversity. *Nordic Journal of Botany* 22: 409–417.

Larsen, K. 2005. Distribution patterns and diversity centres of Zingiberaceae in SE Asia. *Biologiske Skrifter* 55: 219–228.

Larsen, K., J. M. Lock, H. Maas, and P. M. J. Mass. 1998. Zingiberaceae. *In* K. Kubitzki [ed.], The families and genera of vascular plants, vol. 4, Moncotyledons: Alismatanae to Commelinanae (except Gramineae), 474–495. Springer, Berlin, Germany.

Larsen, K., and J. Mood. 1998. *Siamanthus*, a new genus of Zingiberaceae from Thailand. *Nordic Journal of Botany* 18: 393–397.

Larsen, K., and R. M. Smith. 1972. Notes on *Caulokaempferia*. *Notes from the Royal Botanic Garden Edinburgh* 31: 287–295.

Leong-Škorničková, J., L. Ngọc-Sâm, A. D. Poulsen, J. Tosh, and A. Forrest. 2011. *Newmania*: A new ginger genus from central Vietnam. *Taxon* 60: 1386–1396.

Leong-Škorničková, J., O. Šída, E. Záveská, and K. Marhold. 2015. History of infrageneric classification, typification of supraspecific names and outstanding transfers in *Curcuma* (Zingiberaceae). *Taxon* 64: 362–373.

Liao, J. P., and Q. G. Wu. 1996. The significance of the seed anatomy of Chinese *Alpinia*. *In* T. L. Wu, Q.G. Wu, and Z.Y. Chen [eds.], Proceedings of the 2nd Symposium on the Family Zingiberaceae, 92–106. Zhongshan University Press, Guangzhou, China.

Liao, J. P., and Q. G. Wu. 2000. A preliminary study of the seed anatomy of Zingiberaceae. *Botanical Journal of the Linnean Society* 134: 287–300.

MacDowell, A. A., D. Y. Parkinson, A. Haboub, E. Schaible, J. R. Nasiatka, C. A. Yee, J. R. Jameson, et al. 2012. X-ray micro-tomography at the advanced light source. *Proceedings of the Society for Photo-Instrumentation Engineers* 8506: 850618.

Maddison, W. P., and D. R. Maddison. 2015. Mesquite: A modular system for evolutionary analysis, version 3.03 for Windows. Computer program and documentation distributed by the authors, website http://mesquiteproject.org [accessed 30 April 2015].

Manchester, S. R., and W. J. Kress. 1993. *Ensete oregonense* sp. nov. from the Eocene of western North America and its phylogeographic significance. *American Journal of Botany* 80: 1264–1272.

Marone, F., B. Münch, and M. Stampanoni. 2010. Fast reconstruction algorithm dealing with tomography artifacts. SPIE Proceedings, Developments in X-ray tomography VII: 780410.

Marone, F., and M. Stampanoni. 2012. Regridding reconstruction algorithm for real-time tomographic imaging. *Journal of Synchrotron Radiation* 19: 1029–1037.

Mauritzon, J. 1936. Samenbau und Embryologie einiger Scitamineen. *Lunds Universitets Arsskrift* 31: 1–31.

Mood, J. D. 1996. The native gingers of Sabah. *Bulletin of the Heliconia Society International* 8: 1–8.

Mood, J. D., J. F. Veldkamp, S. Dey, and L. M. Prince. 2014. Nomenclatural changes in Zingiberaceae: *Caulokaempferia* is a superfluous name for *Monolophus* and *Jirawongsea* is reduced to *Boesenbergia*. *Gardens' Bulletin Singapore* 66: 215–231.

Netolitzky, F. 1926. Anatomie der Angiospermen-Samen. *In* K. Linsbauer [ed.], Handbuch Pflanzen Anatomie, vol. 10, 1–364. Gebrüder Borntraeger, Berlin, Germany.

Ngamriabsakul, C., M. F. Newman, and Q. C. B. Cronk. 2004. The phylogeny of tribe Zingibereae (Zingiberaceae) based on ITS (nrDNA) and *trnL-F* (cpDNA) sequences. *Edinburgh Journal of Botany* 60: 483–507.

Pedersen, L. B. 2004. Phylogenetic analysis of the subfamily Alpinioideae (Zingiberaceae), particularly *Etlingera* Giseke, based on nuclear and plastid DNA. *Plant Systematics and Evolution* 245: 239–258.

Rangsiruji, A., M. F. Newman, and Q. C. B. Cronk. 2000. A study of the infrageneric classification of *Alpina* (Zingiberaceae) based on the ITS region of nuclear rDNA and the trnL-F spacer of chloroplast DNA. *In* K. L. Wilson and D. A. Morrison [eds.], Monocots: Systematics and evolution, 695–709. CSIRO Publishing, Collingwood, Australia.

Ridley, H. N. 1909. Fruit of *Burbidgea*. *Journal of the Straits Branch of the Royal Asiatic Society* 53: 175–176.

Schumann, K. 1904. Zingiberaceae. *In* A. Engler [ed.], Das Pflanzenreich, vol. IV(46), 1–458. Englemann, Leipzig, Germany.

Simpson, M. G. *2010.* Plant systematics, 2nd ed. Elsevier, Amsterdam, Netherlands.

Smith, S. Y., M. E. Collinson, P. J. Rudall, D. A. Simpson, F. Marone, and M. Stampanoni. 2009. Virtual taphonomy using synchrotron tomographic microscopy reveals cryptic features and internal structure of modern and fossil plants. *Proceedings of the National Academy of Sciences, USA* 106: 12013–12018.

Stampanoni, M., A. Groso, A. Isenegger, G. Mikuljan, Q. Chen, A. Bertrand, S. Henein, et al. 2006. Trends in synchrotron-based tomographic imaging: The SLS experience. *Proceedings of the Society for Photo-Instrumentation Engineers* 6318: 63180M.

Takano, A., and H. Nagamasu. 2007. *Myxochlamys* (Zingiberaceae), a new genus from Borneo. *Acta Phytotaxonomica et Geobotanica* 58(1): 19–32.

Takhtajan, A. 1985. Comparative anatomy of seeds, vol I, 1–318. Izdat Nauka, Leningrad, Russia.

Tschirch, A. 1891. Physiologische Studien uber die Samen, inbesondere die Saugorgane derselben. *Annales du Jardin botanique de Buitenzorg* 8(1): 143–145.

The Plant List. 2013. Version 1.1. Website http://www.theplantlist.org/ [accessed 22 May 2015].

Thiers, B. 2015 [continuously updated]. Index Herbariorum: A global directory of public herbaria and associated staff. New York Botanical Garden's Virtual Herbarium. Available at http://sweetgum.nybg.org/ih/ [accessed 01 January 2015]

Vaughan, J. G. 1970. The structure and utilization of oil seeds. Chapman and Hall, London, UK.

Wada, S., J. A. Kennedy, and B. M. Reed. 2011. Seed-coat anatomy and proanthocyanidins contribute to the dormancy of *Rubus* seed. *Scientia Horticulturae* 130: 762–768.

Williams, K. J., W. J. Kress, and P. S. Manos. 2004. The phylogeny, evolution and classification of the genus *Globba* and tribe Globbeae (Zingiberaceae): Appendages do matter. *American Journal of Botany* 91: 100–114.

Wood, T. H., W. M. Whitten, and N. H. Williams. 2000. Phylogeny of *Hedychium* and related genera (Zingiberaceae) based on ITS sequence data. *Edinburgh Journal of Botany* 57: 261–270.

Wu, M., W. Zhang, P. Guo, and Z. Zhao. 2014. Identification of seven Zingiberaceous species based on comparative anatomy of microscopic characteristics of seeds. *Chinese Medicine* 9(10): 1–7.

Wu, Q. G., and J. P. Liao. 1995. Anatomy and histochemistry of the seeds of *Amomum villosum*. *Journal of Tropical and Subtropical Botany* 3: 52–59.

Xia, Y. M., W. J. Kress, and L. M. Prince. 2004. A phylogenetic analysis of *Amomum* (Alpinioideae: Zingiberaceae) using ITS and *mat*K DNA sequence data. *Systematic Botany* 29: 334–344.

Záveská, E., T. Fér, O. Šída, K. Krak, K. Marhold, and J. Leong–Škorničková. 2012. Phylogeny of *Curcuma* (Zingiberaceae) based on plastid and nuclear sequences: Proposal of the new subgenus *Ecomata*. *Taxon* 61: 747–763.